Representation of High-Dimensional, Molecular Solid-Liquid Phase Diagrams

Ketan D. Samant, David A. Berry, and Ka M. Ng
Dept. of Chemical Engineering, University of Massachusetts, Amherst, MA 01003

A generic framework for the representation of multicomponent molecular solid-liquid phase diagrams in the form of digraphs is presented. Pure components, eutectic points, and saturation points in the solid-liquid composition space are represented as vertices of the digraph. These vertices are connected to form edges on the basis of the adjacency matrix, which is constructed by following a set of generic rules derived from the Gibbs phase rule. These edges form the boundaries of high-dimensional saturation varieties. Included in the framework is a procedure for plotting high-dimensional isobaric and isothermal isobaric phase behavior in the form of projections and cuts. With this framework, solid-liquid phase behavior of multicomponent systems can be easily represented and studied. Applications include facilitation of experimental development of high-dimensional phase diagrams and synthesis of crystallization-based separation processes. The latter is illustrated with the separation of a quinary mixture.

Introduction

Crystallization plays a significant role in the separation of multicomponent organic and inorganic mixtures (Myerson, 1993; Mullin, 1993; Rousseau, 1994). Examples include the recovery of adipic acid from other dibasic acids, meta-xylene from its isomers, potassium chloride, borax, soda ash, sodium sulfate from the salts in Searle Lake, potash from sylvinite, among others. Systematic methods have been developed for the conceptual design of crystallization-based separation processes; most methods rely on visualization of the solid-liquid phase diagram of the system under consideration. After identifying the salient features such as eutectic points, saturation points, eutectic troughs, eutectic surfaces, as well as other saturation varieties, flow sheets can be constructed to completely separate the solutes with suitable operations such as temperature swing, solvent swing, liquid-liquid phase split and reactions (Fitch, 1970; Cisternas and Rudd, 1993; Dye and Ng 1995a,b; Berry et al., 1997; Berry and Ng, 1997; Thomsen et al., 1998). (Readers unfamiliar with the terminology of the features in solid-liquid phase diagrams are referred to these references.)

Correspondence concerning this article should be addressed to K. M. Ng at the Dept. of Chemical Engineering, Hong Kong University of Science and Technology, Clear Water Bay, Hong Kong.
Current address of K. D. Samant: Aspen Technology, Inc., Ten Canal Park, Cambridge, MA 02141-2201.

However, most of these design methods are limited to four components or fewer. The major conceptual impediment is the representation of high-dimensional phase diagrams. As the number of components exceed what can be represented in a three-dimensional (3-D) plot, it is difficult to depict the solid-liquid phase behavior. A perusal of the literature reveals that, even with a great deal of insight and imagination, few studies venture beyond quinary systems (Ricci, 1951; Hasse and Schönert, 1969). The objective of this article is to formulate a generic framework for the representation of simple-eutectic molecular systems with any number of components.

The phase behavior is represented in the form of directed graphs (digraphs) and the associated matrices. In the following, we begin with a discussion of some preliminary concepts and properties regarding this representation. Then, we address the issue of graphical representation of phase diagrams. While it is impossible to view a phase diagram with four or more dimensions, appropriate use of projections and cuts is suggested here to facilitate the formation of a mental picture of the phase diagram in its entirety. A systematic procedure for generating such projections and cuts is described next. Options for identifying and locating the vertices, rules for constructing the adjacency matrices, and options for calculating the edges are discussed. Finally, we describe how to iden-

tify various saturation varieties on the projections and cuts of the phase behavior.

This framework is illustrated with two examples: a quaternary system and a quinary system. In addition, the utility of the framework for crystallization process synthesis is demonstrated with separation of solutes from a quinary system.

Properties of Digraphs Representing Solid-Liquid Phase Diagrams

A *graph* $G=(V, E)$ is a discrete mathematical model consisting of a set of vertices V and a set of edges E joining these vertices. A *digraph* is a graph in which each edge $e_{ij}=(v_i, v_j)$ has a direction from its "initial point" i to its "terminal point" j. In this framework, high-dimensional phase diagrams are represented as digraphs, which in turn can be represented in the form of matrices. The most useful is the adjacency matrix defined as follows (Biggs, 1993).

Definition. (Adjacency Matrix, $A=(a_{ij})$, of a digraph G)

$$a_{ij}=\begin{cases}1 & \text{if } G \text{ has a directed edge } e_{ij}=(v_i, v_j)\\ 0 & \text{else}\end{cases} \tag{1}$$

The row and column headings of the adjacency matrix correspond to the vertices of the digraph. This matrix contains information on how these vertices are connected, or in other words how it indicates the edges of the digraph.

For molecular solid-liquid phase diagrams, pure components, eutectic points, and saturation points form the vertices of the digraph. These vertices are connected by edges, which bound various saturation varieties. For example, on an isobaric phase diagram, a pure component is connected to a binary eutectic by a eutectic trough, a binary eutectic is connected to a ternary eutectic by a binary eutectic trough, and so on. For solid-liquid phase diagrams, the vertices and the edges possess a number of useful properties, which we will now discuss.

At any vertex or along any edge, according to Gibbs phase rule, we have

$$f=W-Q. \tag{2}$$

Here, f represents the degrees of freedom, W the number of intensive variables, and Q the number of equations. For molecular systems, the set of equations consists only of phase equilibrium relations. For example, for p solids in equilibrium with the solution, we have $p+1$ equations. Let us now consider an edge $e_{ij}=(v_i, v_j)$ such that components 1 to m are present along this edge, and of these m components, components 1 to n are saturated. The following axioms and theorems summarize the properties of these vertices and edges. The discussion refers to vertex v_i, but vertex v_j can be considered similarly.

Axiom 1. *The vertices have zero degrees of freedom and the edges have one degree of freedom.*

$$f_{v_i}=W_{v_i}-Q_{v_i}=0 \tag{3a}$$

$$f_{e_{ij}}=W_{e_{ij}}-Q_{e_{ij}}=1 \tag{3b}$$

$$\Rightarrow \left(W_{v_i}-W_{e_{ij}}\right)=\left(Q_{v_i}-Q_{e_{ij}}\right)-1 \tag{3c}$$

Axiom 2. *v_i cannot contain any component other than components 1 to m that are present along e_{ij}.*

Theorem 1. *Components 1 to n that are saturated along e_{ij} are also saturated at v_i. In addition to these n components, v_i can have at most one other saturated component.*

Proof. The equations satisfied on e_{ij} must also be satisfied on v_i since v_i is a part of e_{ij}. Therefore, components 1 to n that are present along e_{ij} must also be saturated at v_i. From axiom 1, $f_{v_i}=f_{e_{ij}}-1=0$. The one less degree of freedom at v_i could be due to the presence of an additional phase equilibrium equation. Thus, in addition to these n components, v_i can have at most one other saturated component.

Theorem 2. *If only components 1 to n are saturated at v_i then the total number of components at v_i is less than m (and equal to $m-1$).*

Proof. Components 1 to n are the only components saturated at v_i. This implies that $Q_{v_i}-Q_{e_{ij}}=0$. Therefore, from axiom 1, $W_{v_i}=W_{e_{ij}}-1$. This implies that v_i has one less variable (which can only be a component mole fraction) than e_{ij}.

Theorem 3. *If v_i has one additional saturated component, then it must contain all m components present along e_{ij}.*

Proof. As v_i has one additional saturated component, $Q_{v_i}-Q_{e_{ij}}=1$. Therefore, from axiom 1, $W_{v_i}=W_{e_{ij}}$. This implies that v_i must contain all the components present along e_{ij}.

Representation of Solid-Liquid Phase Diagrams

Graphical representation

Let us discuss next the various means of graphically representing the phase behavior of a high-dimensional system. Since the solid-liquid phase behavior is insensitive to changes in pressure, we do not consider the effect of pressure in this study.

The isobaric solid-liquid phase diagram for a c-component system is c-dimensional; with $(c-1)$ mole fraction axes and one temperature axis. For high-dimensional systems ($c>3$), these phase diagrams cannot be plotted in two dimensions in their original form. In order to form a mental picture of the high-dimensional diagram, we need to reduce the dimensionality of the system through proper use of projections and cuts. A *projection* is generated by not plotting the effect that one (or more) intensive variable has on the phase behavior. The effect that these variables have on the phase behavior can be evaluated either by using the equations used to calculate the phase behavior or from other projections that do not neglect this effect. Therefore, by definition, a projection contains all the information about the phase behavior although some part of this information is not explicitly represented. A *cut* is generated by plotting the phase behavior at fixed values of one or more intensive variables. Each specified variable reduces the dimensionality of the system by one. A cut provides information about the phase behavior only at these specified values.

The different ways of graphically representing high-dimensional phase diagrams are shown in Figure 1. For $c \geq 3$, to make the graphical representation of the isobaric phase behavior more useful, the temperature coordinate is eliminated first. This can be done in two ways as shown in Figure 1. In

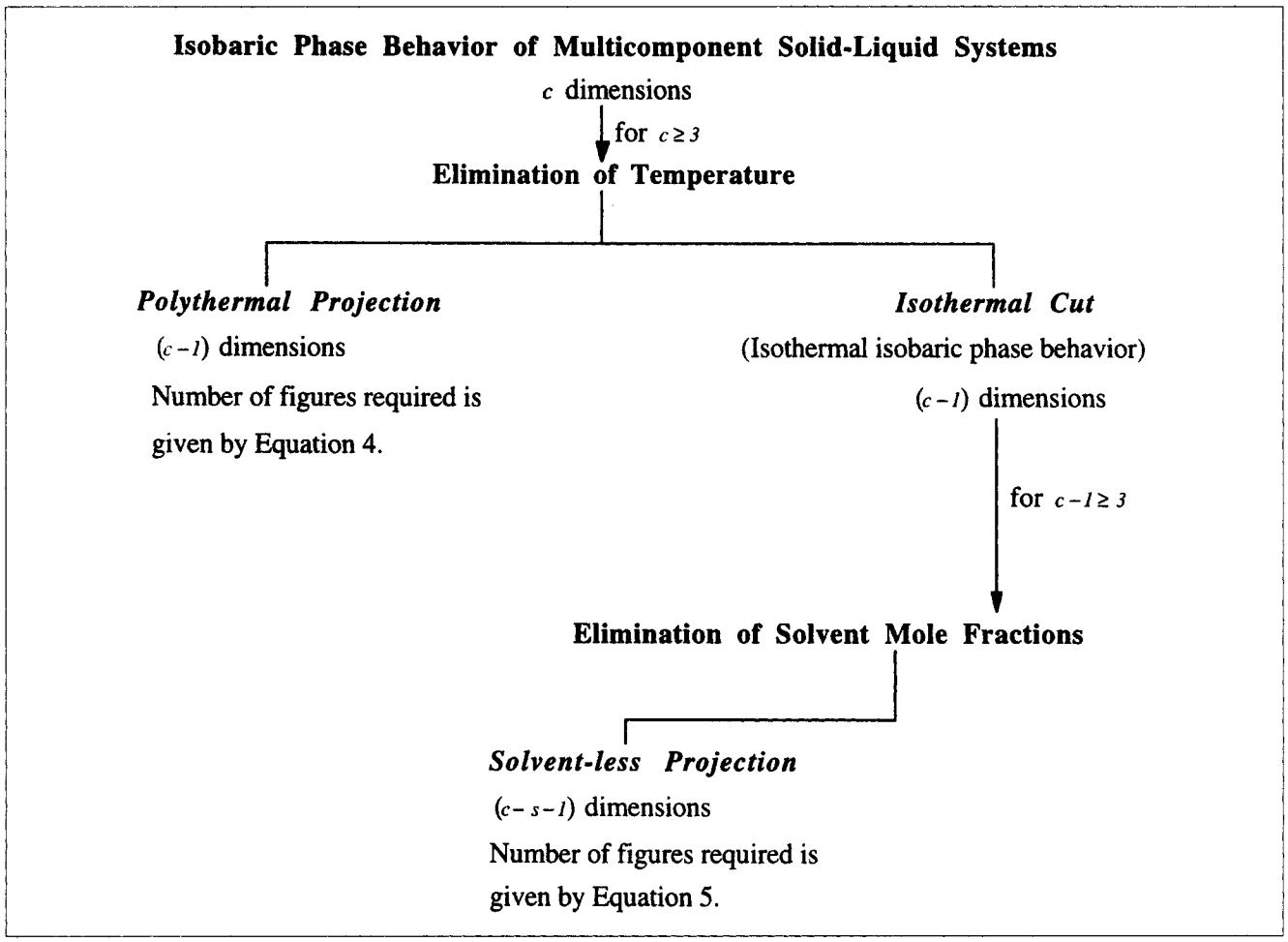

Figure 1. Graphical representation of phase diagrams.

the first method, the phase diagram is plotted by ignoring the effect of temperature. This gives rise to the *polythermal projection*. The polythermal projection has $c-1$ dimensions. Therefore, for $c \geq 4$, it is still not possible to plot the phase diagrams in two dimensions. In this situation, we can plot the phase diagram by selecting three components at a time and ignoring the effect of the mole fractions of the remaining $c-3$ components. (Note that the mole fractions of the three selected components have to be normalized so that they add up to unity, and a figure plotted in this manner is called a *Jänecke projection.*) On any Jänecke projection, the saturation varieties comprising these $c-3$ components cannot be plotted and the representation is incomplete. Therefore, clearly, more than one Jänecke projection is needed for completely representing the phase behavior. We can plot $\binom{c}{3}$ such figures. However, not all are required for complete representation of the phase behavior. The minimum number for this task is given by

$$P = \left(\frac{c-1}{2}\right)^2 + k, \quad k = \begin{cases} 0 & \text{if } c \text{ is odd} \\ 3/4 & \text{if } c \text{ is even} \end{cases}. \qquad (4)$$

The derivation of this equation is provided in the Appendix. The Jänecke projections have to be selected as discussed in this derivation. The remaining $\binom{c}{3} - P$ Jänecke projections do not offer any additional information. However, whenever necessary, they may be used as supplementary information.

In the second method, the phase diagram is plotted at a specified temperature. This *isothermal cut* represents the isothermal isobaric phase behavior of the system at the specified temperature. Similar to the polythermal projection, for $c \geq 4$, the isothermal cut has to be plotted as multiple figures (minimum number being given by Eq. 4). In some cases, we can reduce the dimensionality further by eliminating the mole fractions of the solvents. Solvents are the components that, at the specified temperature, exist in liquid phase only. Note that a *solvent-less* projection is a Jänecke projection. If at the specified temperature we have s solvents, the solvent-less projection reduces the dimensionality to $c-s-1$. Again, for $c-s \geq 4$ we need more than one figure to plot the solvent-less projections completely. The minimum number of figures (see Appendix) is given by

$$P = \left(\frac{c-s-1}{2}\right)^2 + k, \quad k = \begin{cases} 0 & \text{if } c-s \text{ is odd} \\ 3/4 & \text{if } c-s \text{ is even} \end{cases}. \qquad (5)$$

For a given multicomponent system, depending on the application, any of these projections or cuts may be used to

study the phase behavior. However, to plot them, we need to know the vertices and the edges of the digraphs that represent the isobaric and isothermal isobaric phase behavior. In the following subsection, we discuss a systematic procedure for this task.

Systematic procedure for constructing the digraphs

This systematic procedure comprises three steps, each of which is discussed below. We denote the isobaric phase diagram of multicomponent molecular systems by a digraph $G_P^M = (V_P^M, E_P^M)$ and the isothermal isobaric phase diagram by a digraph $G_{PT}^M = (V_{PT}^M, E_{PT}^M)$. Subscripts P and T indicate constant pressure and temperature, respectively. The superscript M refers to molecular systems.

Step 1: Identification and Location of the Vertices. For isobaric phase diagrams of molecular systems, pure components and eutectic points form the set of vertices. Saturation points form the vertices of the isothermal isobaric phase diagram. The saturation points that can exist on an isothermal isobaric phase diagram are determined by identifying the intersection points of the specified temperature plane with the edges of the isobaric phase diagram. Irrespective of the type of the phase diagram, the vertices are labeled after the saturated components. Unsaturated components, if present, are written as subscripts. For example, the vertex at which components A and B are saturated is labeled as AB and vertex AB_C indicates that components A and B are saturated and component C is unsaturated at this vertex. The location of vertices refers to the values of intensive variables associated with the vertices. For a given system, the location of pure component vertices must be specified. Locations of eutectic and saturation points can then be determined by using appropriate methods based on the input information. Let us now discuss these methods.

(1) Isobaric Phase Behavior. The set of vertices V_P^M comprises the pure components and the eutectic points. Therefore, we have $\sum_{i=1}^{c} \binom{c}{i}$ vertices for a c-component system. To determine the location of each vertex, we need to know its composition and temperature. The pure component compositions and melting points ($T_{m,i}$) are known. The eutectic compositions and temperatures can be estimated either experimentally or from phase equilibrium equations of the form

$$\sum_{i=1}^{k} x_i^{\text{sat}} = 1; \quad x_i^{\text{sat}} = \frac{1}{\gamma_i} \exp\left[\frac{\Delta H_{m,i}^o}{R}\left(\frac{1}{T_{m,i}} - \frac{1}{T}\right)\right] \tag{6}$$

This equation corresponds to a eutectic point at which solids 1 to k coexist with the liquid of the same composition. To locate the vertices using this equation, we need the pure component data ($T_{m,i}$, $\Delta H_{m,i}^o$) and a thermodynamic model for the liquid phase activity coefficients (γ_i). Typically, only the pure component data are available. In such cases, we can locate the eutectic points by assuming the system to be ideal ($\gamma_i = 1$, $\forall i$). The locations so determined can be used as starting points for their experimental determination.

(2) Isothermal Isobaric Phase Behavior. The vertices $\in V_{PT}^M$ are identified after completing all three steps of this procedure for G_P^M. First, we rewrite the adjacency matrix of G_P^M (construction of adjacency matrices will be discussed in detail in step 2) such that the row and column headings are now arranged in decreasing order of temperature. Then, we identify the lowest row (and column) index k for which the temperature has a value lower than the specified temperature and modify the adjacency matrix as

$$\begin{aligned} a_{ij} &= 0 \quad \forall i < k \quad \text{and} \quad j < k \\ a_{ij} &= 0 \quad \forall i \geq k \quad \text{and} \quad j \geq k \end{aligned} \tag{7}$$

For a c-component system, the adjacency matrix as modified above may have two nonzero parts; viz., the upper righthand corner matrix of order $(k-1)\times(\sum_{i=1}^{c}\binom{c}{i} - k + 1)$ and the lower lefthand corner matrix of order $(\sum_{i=1}^{c}\binom{c}{i} - k + 1)\times(k-1)$. If $a_{ij} = 1$ within these nonzero parts, we say we have a point of intersection between vertices $v_i \in V_P^M$ and $v_j \in V_P^M$. This point of intersection forms a vertex $\in V_{PT}^M$ and lies on the edge $\in E_P^M$ that connects v_i and v_j. The components common to $v_i \in V_P^M$ and $v_j \in V_P^M$ are saturated at this new vertex and the remaining component is unsaturated.

To locate the vertices thus identified, we need to determine the component mole fractions at these vertices at the specified temperature. This can be done by using the functional relationships describing the edges $\in E_P^M$ on which these vertices are located (different options of calculating the edges $\in E_P^M$ will be discussed in step 3). For example, if the edges $\in E_P^M$ are straight lines, then a new vertex $v^* \in V_{PT}^M$ lying on $e_{ij} \in E_P^M$ is located as

$$\boldsymbol{x}(v^*) = f\boldsymbol{x}(v_i) + (1-f)\boldsymbol{x}(v_j); \quad f = \frac{T(v^*) - T(v_j)}{T(v_i) - T(v_j)} \tag{8}$$

and if the edges $\in E_P^M$ are calculated by assuming the system to behave ideally, the new vertex v^* is located as

$$\begin{aligned} x_i(v^*) &= \exp\left[\frac{\Delta H_{m,i}^o}{R}\left(\frac{1}{T_{m,i}} - \frac{1}{T(v^*)}\right)\right] \quad i = 1, \ldots, k, \\ x_{k+1}(v^*) &= 1 - \sum_{i=1}^{k} x_i(v^*) \end{aligned} \tag{9}$$

In Eq. 9, it is assumed that components 1 to k are saturated and component $k+1$ is unsaturated along $e_{ij} \in E_P^M$.

Step 2: Construction of the Adjacency Matrix. Once all the vertices are identified and located, we have to construct the adjacency matrix using the adjacency rules. To develop these rules, we have to determine the conditions under which a vertex v_i is adjacent to another vertex v_j. If v_i is adjacent to v_j, the digraph has an edge $e_{ij} = (v_i, v_j)$ and theorems 1 to 3 are valid for v_i, v_j, and e_{ij}. In view of these theorems, we can consider the following two cases.

Case 1: v_j has more saturated components than v_i:

- According to theorem 1, all components saturated at v_i are saturated along e_{ij} and therefore also at v_j. In addition v_j has one other saturated component.
- According to theorem 2, v_i has one less component than e_{ij}.
- According to theorem 3, v_j has all the components of e_{ij}.

Therefore this case gives rise to the following adjacency rule:

Rule 1. v_i *is adjacent to* v_j *if:*

- v_j has more components than v_i and has all the components in v_i.
- All components saturated at v_i are also saturated at v_j.
- v_j has one additional saturated component.

Case 2: v_j *has the same number of saturated components as* v_i.

- According to theorem 1, the number of components saturated at both v_i and v_j is either the same as the number of components saturated along e_{ij} or is one more than the number of components saturated along e_{ij}.
- If both v_i and v_j have the same number of saturated components as e_{ij} then according to theorem 1, these components are the same and are also saturated along e_{ij}.
- If both v_i and v_j have one more saturated component, then from theorem 3, both should have all the components along e_{ij}. This also implies that both v_i and v_j have the same components, all the components saturated along e_{ij} are also saturated at v_i and v_j, and the additional saturated component at v_i is different than the additional saturated component at v_j.

Therefore this case gives rise to the following two adjacency rules:

Rule 2. v_i *is adjacent to* v_j *if:*

- v_i and v_j have the same number of saturated components.
- All the components saturated at v_i are also saturated at v_j.

Rule 3. v_i *is adjacent to* v_j *if:*

- v_i and v_j have the same components and the same number of saturated components.
- All but one component saturated at v_i are also saturated at v_j.

It is interesting to note here that the rule 1 results in unidirectional edges (v_i is adjacent to v_j, but v_j is not adjacent to v_i), while rules 2 and 3 result in bidirectional edges (v_i is adjacent to v_j and v_j is adjacent to v_i). For isobaric phase behavior, all edges are unidirectional and only rule 1 is applicable. For isothermal isobaric phase behavior, bidirectional edges are possible.

Table 1. Data for the Quaternary System (Example 1)

Pure Component Data					
	ΔH_m^o (J/mol)				T_m (K)
A	30,000				470
B	29,000				460
C	28,000				450
D	23,000				350
Eutectic Compositions and Temperatures					
	x_A	x_B	x_C	x_D	T (K)
Binary					
AB	0.45	0.55	0.0	0.0	426.05
AC	0.41	0.0	0.59	0.0	420.65
AD	0.07	0.0	0.0	0.93	347.02
BC	0.0	0.45	0.55	0.0	416.50
BD	0.0	0.08	0.0	0.92	346.22
CD	0.0	0.0	0.10	0.90	345.25
Ternary					
ABC	0.27	0.33	0.40	0.0	401.19
ABD	0.06	0.08	0.0	0.86	343.64
ACD	0.06	0.0	0.10	0.84	342.75
BCD	0.0	0.07	0.09	0.84	342.07
Quaternary					
ABCD	0.05	0.07	0.09	0.79	339.87

Step 3: Calculation of the Edges. For accurate graphical representation of the phase behavior, it is essential that the edges identified from the adjacency matrix are calculated and plotted as accurately as possible. Let us discuss the various options for this task.

(1) Isobaric Phase Behavior. The edges $\in E_P^M$ can be determined from the adjacency matrix by reading across its rows. As all edges result from application of rule 1, they are unidirectional, directed from the vertex with fewer components to the vertex with more components (that is, in the direction of decreasing temperature). Saturated components common to the vertices that are connected by an edge are also saturated along that edge. Therefore, these edges are described by solid-liquid phase equilibrium equations of the form

$$\sum_{i=1}^{k} x_i^{\text{sat}} = \sum_{i=1}^{k} \frac{1}{\gamma_i} \exp\left[\frac{\Delta H_{m,i}^o}{R}\left(\frac{1}{T_{m,i}} - \frac{1}{T}\right)\right] = 1 - x_{k+1} \quad (10)$$

The above equation represents the edge connecting vertices v_i and v_j such that components 1 to k are saturated at vertex v_i and components 1 to $k+1$ are saturated at vertex v_j. Depending on the availability of information, we can approximate the edges by using any of the following options:

- Joining the vertices by straight lines. This method is incorrect but is useful in getting an idea of the general structure of the phase behavior. For example, if we join the vertices by straight lines and take isothermal cuts, we can determine which saturation varieties will be observed on the isothermal cut and their approximate locations. This knowledge can effectively be used as a guide for obtaining isothermal experimental data which can then be used to get an improved description of the edges.
- Assuming ideal behavior and using pure component melting points and heats of fusion. This method is especially useful if reliable data on eutectic points is not available.
- Assuming predictive models for the activity coefficients. This method is especially useful if such models are well-established or experimental data are available to validate the model parameters.

	A	*B*	*C*	*D*	*AB*	*AC*	*AD*	*BC*	*BD*	*CD*	*ABC*	*ABD*	*ACD*	*BCD*	*ABCD*
A	0	0	0	0	1	1	1	0	0	0	0	0	0	0	0
B	0	0	0	0	1	0	0	1	1	0	0	0	0	0	0
C	0	0	0	0	0	1	0	1	0	1	0	0	0	0	0
D	0	0	0	0	0	0	1	0	1	1	0	0	0	0	0
AB	0	0	0	0	0	0	0	0	0	0	1	1	0	0	0
AC	0	0	0	0	0	0	0	0	0	0	1	0	1	0	0
AD	0	0	0	0	0	0	0	0	0	0	0	1	1	0	0
BC	0	0	0	0	0	0	0	0	0	0	1	0	0	1	0
BD	0	0	0	0	0	0	0	0	0	0	0	1	0	1	0
CD	0	0	0	0	0	0	0	0	0	0	0	0	1	1	0
ABC	0	0	0	0	0	0	0	0	0	0	0	0	0	0	1
ABD	0	0	0	0	0	0	0	0	0	0	0	0	0	0	1
ACD	0	0	0	0	0	0	0	0	0	0	0	0	0	0	1
BCD	0	0	0	0	0	0	0	0	0	0	0	0	0	0	1
ABCD	0	0	0	0	0	0	0	0	0	0	0	0	0	0	0

Figure 2. Adjacency matrix for the isobaric phase diagram of Example 1.

(2) Isothermal Isobaric Phase Behavior. The components that are saturated and unsaturated along the edges $\in E_{PT}^{M}$ can be identified from the vertices that these edges connect. The edges can then be calculated easily by using an appropriate thermodynamic model. Note that these edges are straight lines for ideal systems. In our experience, these edges can simply be assumed to be straight lines, without significant errors, when a thermodynamic model for the liquid phase activity coefficients is not available.

Identification of saturation varieties

The edges of the digraph form the boundaries of various saturation varieties. For the conceptual design of crystalliza-

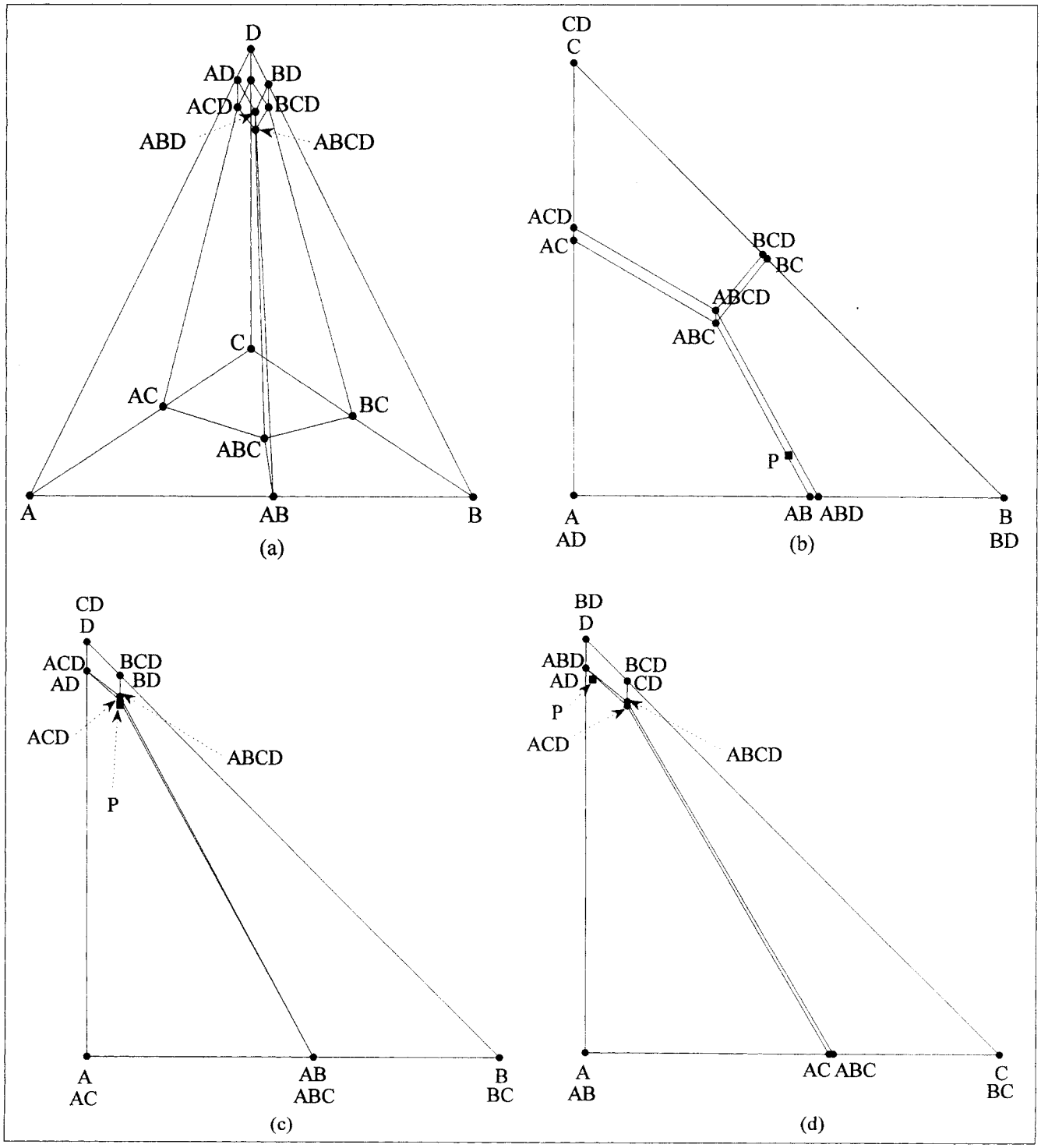

Figure 3. Polythermal projections of the isobaric phase diagram of Example 1.

(a) Tetrahedral polythermal projection; (b), (c), and (d) 2-D representation of the polythermal projection.

Saturation Variety Matrix

	A	B	C	D	AB	AC	AD	BC	BD	CD	ABC	ABD	ACD	BCD	ABCD
A - sat	1	0	0	0	1	1	1	0	0	0	1	1	1	0	1
B - sat	0	1	0	0	1	0	0	1	1	0	1	1	0	1	1
C - sat	0	0	1	0	0	1	0	1	0	1	1	0	1	1	1
D - sat	0	0	0	1	0	0	1	0	1	1	0	1	1	1	1
AB - double sat	0	0	0	0	1	0	0	0	0	0	1	1	0	0	1
AC - double sat	0	0	0	0	0	1	0	0	0	0	1	0	1	0	1
AD - double sat	0	0	0	0	0	0	1	0	0	0	0	1	1	0	1
BC - double sat	0	0	0	0	0	0	0	1	0	0	1	0	0	1	1
BD - double sat	0	0	0	0	0	0	0	0	1	0	0	1	0	1	1
CD - double sat	0	0	0	0	0	0	0	0	0	1	0	0	1	1	1
ABC - triple sat	0	0	0	0	0	0	0	0	0	0	1	0	0	0	1
ABD - triple sat	0	0	0	0	0	0	0	0	0	0	0	1	0	0	1
ACD - triple sat	0	0	0	0	0	0	0	0	0	0	0	0	1	0	1
BCD - triple sat	0	0	0	0	0	0	0	0	0	0	0	0	0	1	1
ABCD - quadruple sat	0	0	0	0	0	0	0	0	0	0	0	0	0	0	1

Figure 4. Saturation variety matrix for the isobaric phase diagram of Example 1.

tion-based separation processes, it is sufficient to just identify these saturation varieties. For more quantitative design methods, we need to express them in the form of linear algebraic equations (Pressly and Ng, 1999). However, it is not apparent from the adjacency matrix, which saturation varieties are bounded by which edges. For this purpose, the saturation variety matrix is more useful. The row headings of this matrix correspond to saturation varieties and the column headings correspond to the vertices of the corresponding digraph. This matrix can be formally defined as follows:

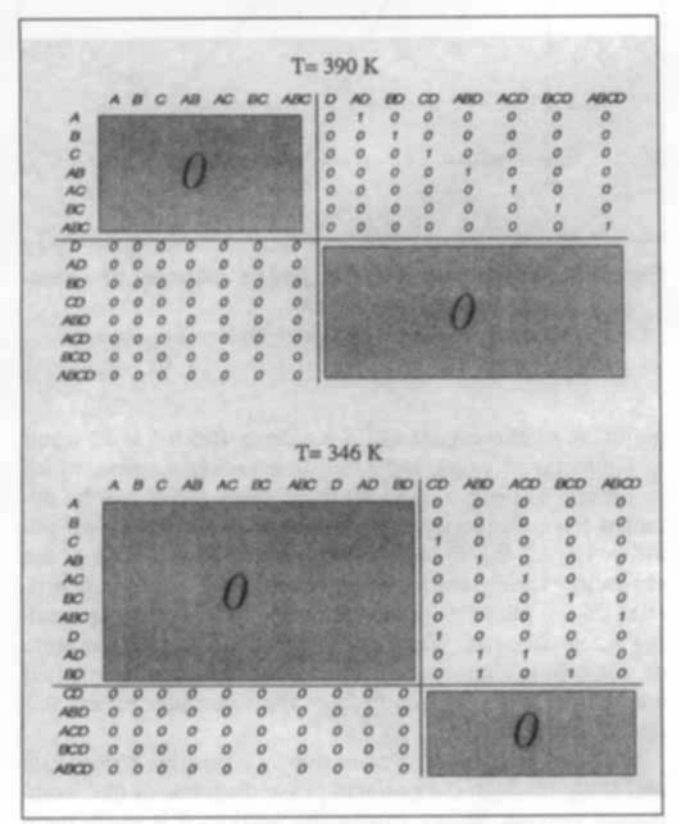

Figure 5. Modified adjacency matrices at 390 K and 346 K.

Definition. (Saturation Variety Matrix, $S = (s_{ij})$)

$$s_{ij} = \begin{cases} 1 & \text{if vertex } v_j \text{ lies on the saturation variety} \\ & \text{represented by row } i \\ 0 & \text{else} \end{cases} \quad (11)$$

For a given digraph, the saturation varieties that are present are obtained from the components saturated at the vertices and along the edges. For example, vertex AB implies the presence of AB-double saturation variety and edge $AB_C - AC_B$ implies the presence of A-saturation variety. To construct S, first the vertices are listed as column headings and all the saturation varieties are listed as row headings. The matrix is then constructed as

$$s_{ij} = \begin{cases} 1 & \text{if all components saturated in the row heading} \\ & \text{are also saturated in the column heading} \\ 0 & \text{else} \end{cases} \quad (12)$$

When the adjacency matrix A is constructed by application of rule 1 only, S can be constructed by algebraic manipulation of A as

$$S = \text{boolean}\left[(A + I)^m\right], \quad (13)$$

Table 2. Location of Vertices of the Isothermal Isobaric Phase Diagrams of Example 1

$T = 390$ K				
Vertex	x_A	x_B	x_C	x_D
A_D	0.21	0.0	0.0	0.79
B_D	0.0	0.26	0.0	0.74
C_D	0.0	0.0	0.32	0.68
AB_D	0.21	0.26	0.0	0.53
AC_D	0.21	0.0	0.32	0.47
BC_D	0.0	0.26	0.32	0.42
ABC_D	0.21	0.26	0.32	0.21
$T = 346$ K				
Vertex	x_A	x_B	x_C	x_D
C_D	0.0	0.0	0.11	0.89
D_C	0.0	0.0	0.09	0.91
AB_D	0.06	0.08	0.0	0.86
AC_D	0.06	0.0	0.11	0.83
AD_B	0.06	0.03	0.0	0.91
AD_C	0.06	0.0	0.03	0.91
BC_D	0.0	0.08	0.11	0.81
BD_A	0.01	0.08	0.0	0.91
BD_C	0.0	0.08	0.01	0.91
ABC_D	0.06	0.08	0.11	0.75

where the boolean operator turns all elements greater than unity to unity. The exponent m is defined as

$$m = c_{\max} - c_{\min}, \tag{14}$$

where $c_{\max}$ and $c_{\min}$, respectively, are the maximum and the minimum number of saturated components in the vertices of the digraph. Note that this is possible as all edges of the digraph are unidirectional and S is square. Rules 2 and 3 result in bidirectional edges and saturation variety matrices which in general are not square. In these cases too S can be obtained from algebraic manipulation of A. However, we will utilize Eq. 12, as it is much more convenient to use. Once the saturation variety matrix is constructed, the saturation varieties on the phase diagrams can easily be identified by reading across its rows. When the composition and temperature of a stream are known, we can identify the components that are saturated in this stream from the saturation variety this stream lies within.

With this framework, we are now in a position to visualize and study the high-dimensional phase diagrams of multicomponent systems. Before closing this section, it is worth mentioning that the adjacency rules are generic and can also be applied to multicomponent reactive, compound forming, and

(a) T = 390 K

	A_D	B_D	C_D	AB_D	AC_D	BC_D	ABC_D
A_D	0	0	0	1	1	0	0
B_D	0	0	0	1	0	1	0
C_D	0	0	0	0	1	1	0
AB_D	0	0	0	0	0	0	1
AC_D	0	0	0	0	0	0	1
BC_D	0	0	0	0	0	0	1
ABC_D	0	0	0	0	0	0	0

(b) T = 346 K

	C_D	D_C	AB_D	AC_D	AD_B	AD_C	BC_D	BD_A	BD_C	ABC_D
C_D	0	0	0	1	0	0	1	0	0	0
D_C	0	0	0	0	0	1	0	0	1	0
AB_D	0	0	0	0	1	0	0	1	0	1
AC_D	0	0	0	0	0	1	0	0	0	1
AD_B	0	0	1	0	0	1	0	1	0	0
AD_C	0	0	0	1	1	0	0	0	0	0
BC_D	0	0	0	0	0	0	0	0	1	1
BD_A	0	0	1	0	1	0	0	0	1	0
BD_C	0	0	0	0	0	0	1	1	0	0
ABC_D	0	0	0	0	0	0	0	0	0	0

Figure 6. Adjacency matrices for the isothermal isobaric phase diagrams of Example 1.

(a) $T = 390$ K; (b) $T = 346$ K.

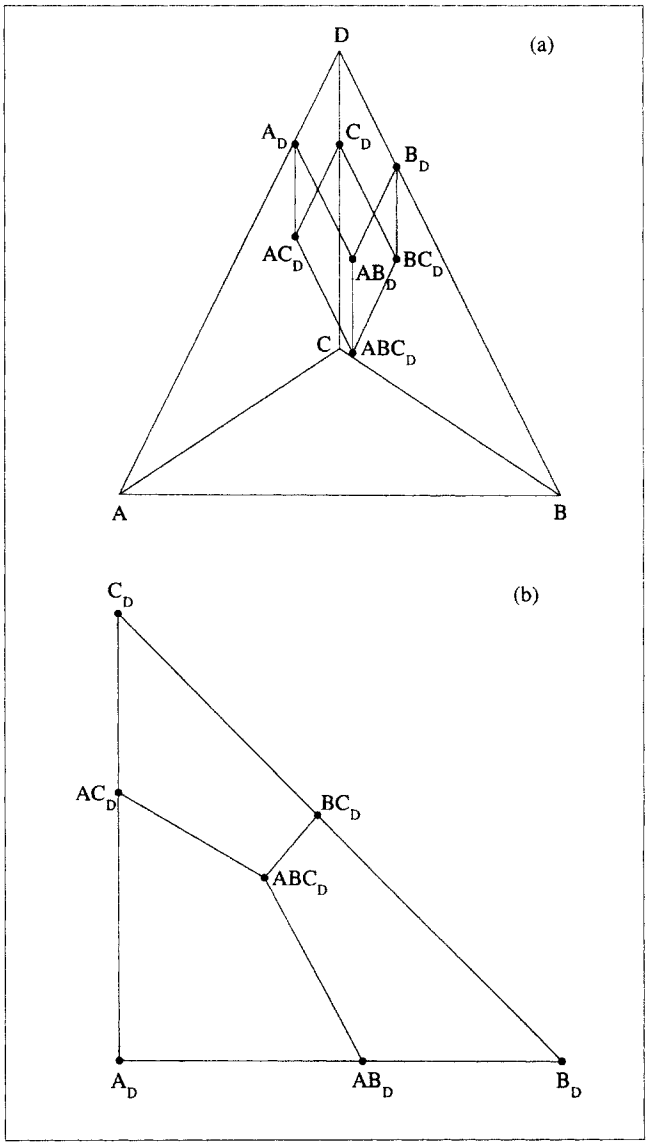

Figure 7. Isothermal isobaric phase diagram of Example 1 at 390 K.

(a) Tetrahedral phase diagram; (b) Jänecke projection.

ionic systems. Let us now consider a few examples to illustrate the above ideas.

Examples

Example 1: quaternary system

Consider a system with components, A, B, C, and D. Only pure component parameters as listed in Table 1 are available. Let us first consider the isobaric phase behavior of this system.

Step 1. There are 15 vertices (4 pure components, 6 binary eutectic points, 4 ternary eutectic points, and 1 quaternary eutectic point). The eutectic compositions and temperatures were calculated by assuming the system to behave ideally. The results of these calculations are also summarized in Table 1.

Step 2. The adjacency matrix for this system is shown in Figure 2. Note, for example, that vertex AB (row heading) is adjacent to vertices ABC and ABD (column headings) according to rule 1 as these vertices have all the components saturated at AB (A and B) and an additional saturated component (C and D, respectively).

Step 3. The adjacency matrix of Figure 2 reveals 28 edges (3 starting from each pure component vertex, 2 starting from each binary eutectic point, and 1 starting from each ternary eutectic point). For example, the edge $AB-ABC$ is directed from AB to ABC and the edge $AB-ABD$ is directed from AB to ABD. These edges are calculated using Eq. 10 by assuming ideal behavior ($\gamma_i = 1, \forall i$).

Figure 3 shows the polythermal projection of the phase diagram. The projection is shown in Figure 3a as a tetrahedral phase diagram. We need three figures to represent this tetrahedral diagram in two dimensions. These are shown in Figures 3b to 3d. In Figure 3b, the mole fraction of component D is not considered and the mole fractions of A, B, and C are normalized to add up to unity. The D-saturation variety cannot be plotted on this diagram as the mole fraction of D is not considered. Similarly, mole fractions of components C and B are not considered in Figures 3c and 3d, respectively. The edges appear as straight lines connecting the vertices as the system was assumed to be ideal and temperature is not plotted.

The maximum number of saturated components is $c_{max} = 4$ (components A, B, C, and D at vertex $ABCD$) and the minimum number of saturated components is $c_{min} = 1$ (at the pure component vertices). With $m = 3$, the saturation variety matrix is as shown in Figure 4. The edges bounding various saturation varieties can be identified from this matrix by simply reading across its rows. For example, the A-saturation variety can be identified by reading across row A as the region enclosed by the edges connecting A, AB, AC, AD, ABC, ABD, ACD, and $ABCD$. Similarly, the ABC-triple saturation variety can be identified by reading across row ABC as the edge joining ABC and $ABCD$, and so on.

Now let us consider the isothermal isobaric phase behavior at two values of temperature, 390 K and 346 K.

Step 1. Figure 5 shows the adjacency matrix of Figure 2 modified as discussed at these two temperatures. For the isothermal cut at 390 K, we have seven new vertices, viz., A_D, B_D, C_D, AB_D, AC_D, BC_D, and ABC_D. Components A, B, and C are solutes as they can exist in solid phase, while D is a solvent as it does not appear as a saturated component in the new vertices. At 346 K we have ten new vertices, viz., C_D, D_C, AB_D, AC_D, AD_B, AD_C, BC_D, BD_A, BD_C, and ABC_D. At this temperature, all components can exist in solid phase. Therefore, no component can be designated as a solvent. The locations of the vertices at both temperatures are listed in Table 2. These locations are calculated by assuming ideal behavior.

Step 2. At 390 K, rule 1 is sufficient to construct the adjacency matrix. For example, vertex A_D is adjacent to vertices AB_D and AC_D and vertex AB_D is adjacent to vertex ABC_D according to rule 1. The new adjacency matrix is shown in Figure 6a. At 346 K, all three rules are needed to construct the adjacency matrix. For example, vertex C_D is adjacent to vertex AC_D according to rule 1, vertex BD_A is adjacent to vertex BD_C (and vice versa) as per rule 2, and vertex AB_D is adjacent to vertex AD_B (and vice versa) by rule 3. The new adjacency matrix at 346 K is shown in Figure 6b.

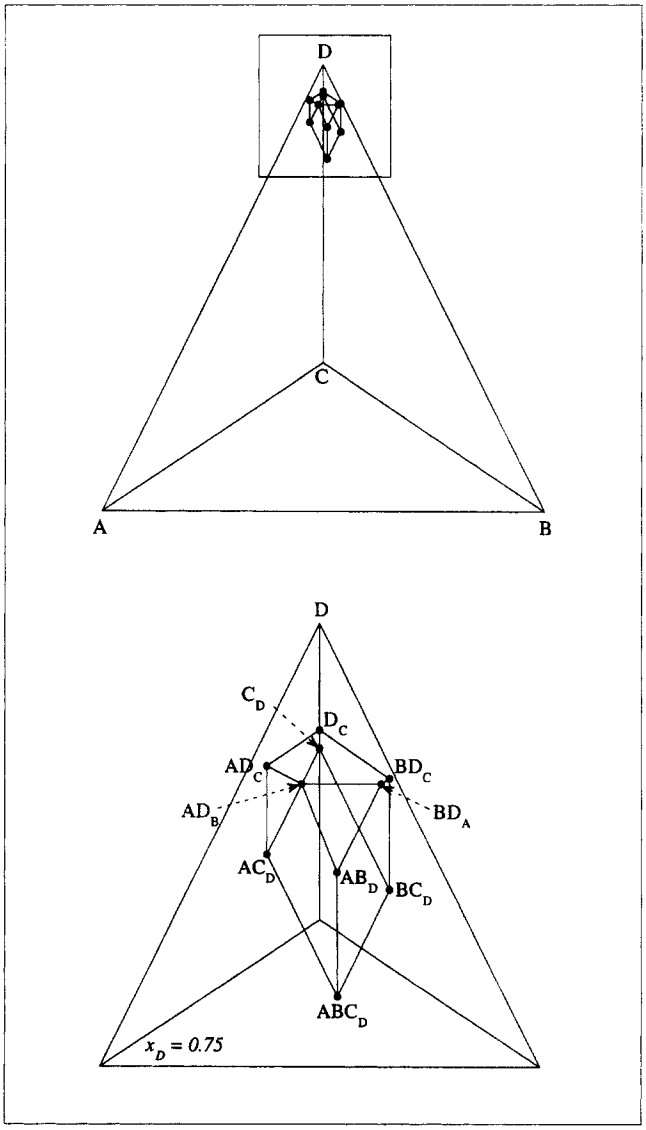

Figure 8. Isothermal isobaric phase diagram of Example 1 at 346 K.

Step 3. The adjacency matrices at 390 K and 346 K (Figures 6a and 6b) reveal 9 and 14 edges, respectively. As we have assumed the system to behave ideally, the edges are simply straight lines. Again, the edges formed by application of rule 1 are unidirectional and the edges formed by application of rules 2 and 3 are bidirectional. Therefore, all the edges at 390 K are unidirectional, whereas at 346 K, some edges like $BD_A - BD_C$ and $AB_D - AD_B$ are bidirectional.

Figure 7a shows the tetrahedral plot of the isothermal isobaric phase diagram at 390 K. As component D is a solvent, we can plot the Jänecke projection by ignoring the mol fraction of D and normalizing the mol fractions of A, B, and C so that they add up to unity. This Jänecke projection is shown in Figure 7b. Figure 8 shows the tetrahedral plot of the isothermal isobaric phase diagram at 346 K. In this case, we do not have any component designated as a solvent. Therefore, we need three figures (Figures 9a to 9c) to plot the projections of the phase diagram in two dimensions. In Figures 9a 9b, and 9c, mol fractions of components B, C, and D, respectively, are not plotted.

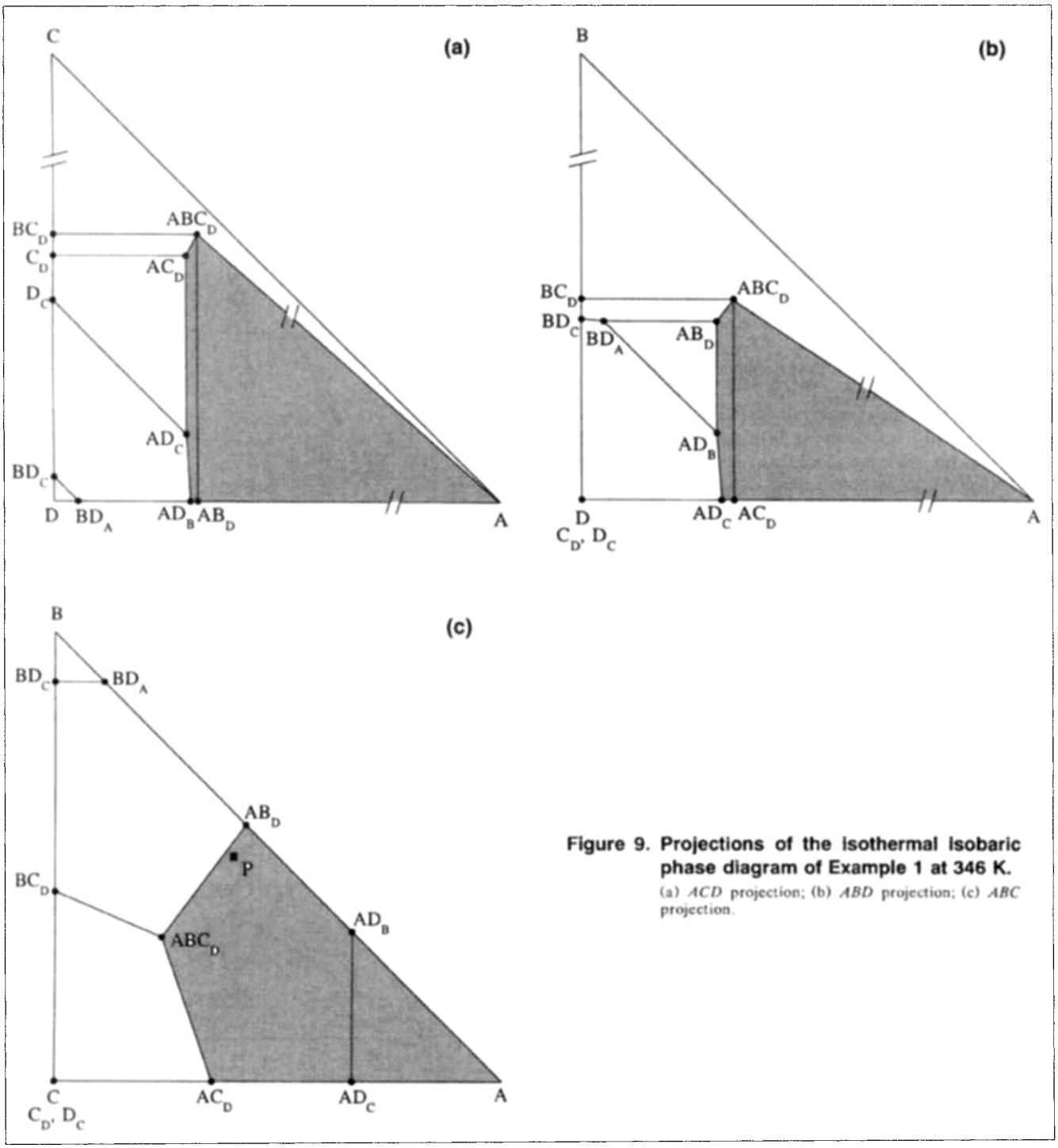

Figure 9. Projections of the isothermal isobaric phase diagram of Example 1 at 346 K.

(a) *ACD* projection; (b) *ABD* projection; (c) *ABC* projection.

(a) T = 390 K

	A_D	B_D	C_D	AB_D	AC_D	BC_D	ABC_D
A - sat	1	0	0	1	1	0	1
B - sat	0	1	0	1	0	1	1
C - sat	0	0	1	0	1	1	1
AB - double sat	0	0	0	1	0	0	1
AC - double sat	0	0	0	0	1	0	1
BC - double sat	0	0	0	0	0	1	1
ABC - triple sat	0	0	0	0	0	0	1

(b) T = 346 K

	C_D	D_C	AB_D	AC_D	AD_B	AD_C	BC_D	BD_A	BD_C	ABC_D
A - sat	0	0	1	1	1	1	0	0	0	1
B - sat	0	0	1	0	0	0	1	1	1	1
C - sat	1	0	0	1	0	0	1	0	0	1
D - sat	0	1	0	0	1	1	0	1	1	0
AB - double sat	0	0	1	0	0	0	0	0	0	1
AC - double sat	0	0	0	1	0	0	0	0	0	1
AD - double sat	0	0	0	0	1	1	0	0	0	0
BC - double sat	0	0	0	0	0	0	1	0	0	1
BD - double sat	0	0	0	0	0	0	0	1	1	0
ABC - triple sat	0	0	0	0	0	0	0	0	0	1

Figure 10. Saturation variety matrices for the isothermal isobaric phase diagrams of Example 1.

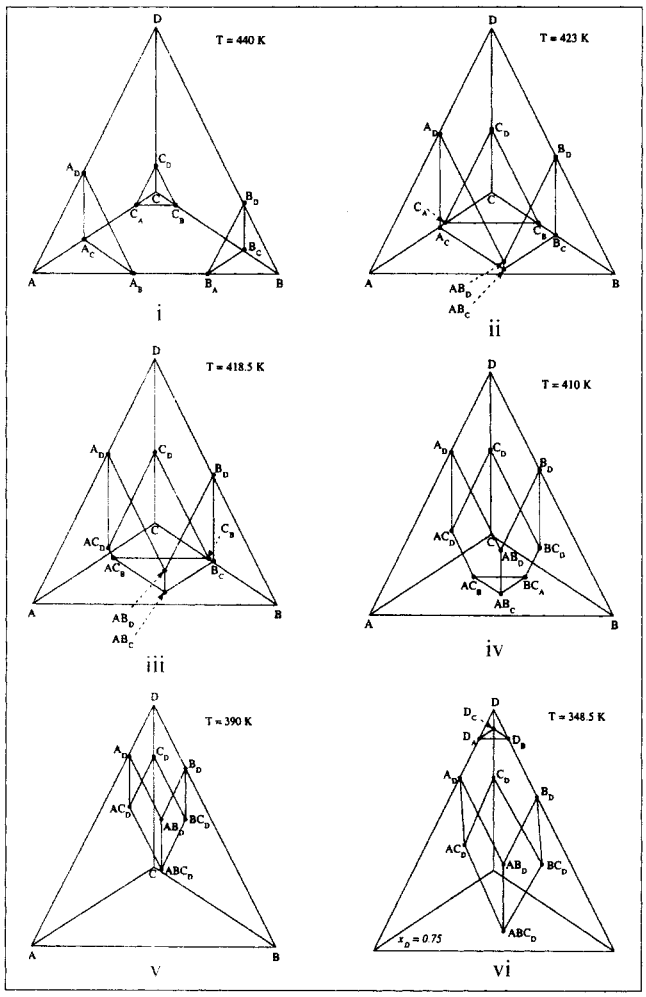

Figure 11. Evolution of saturation varieties for Example 1.

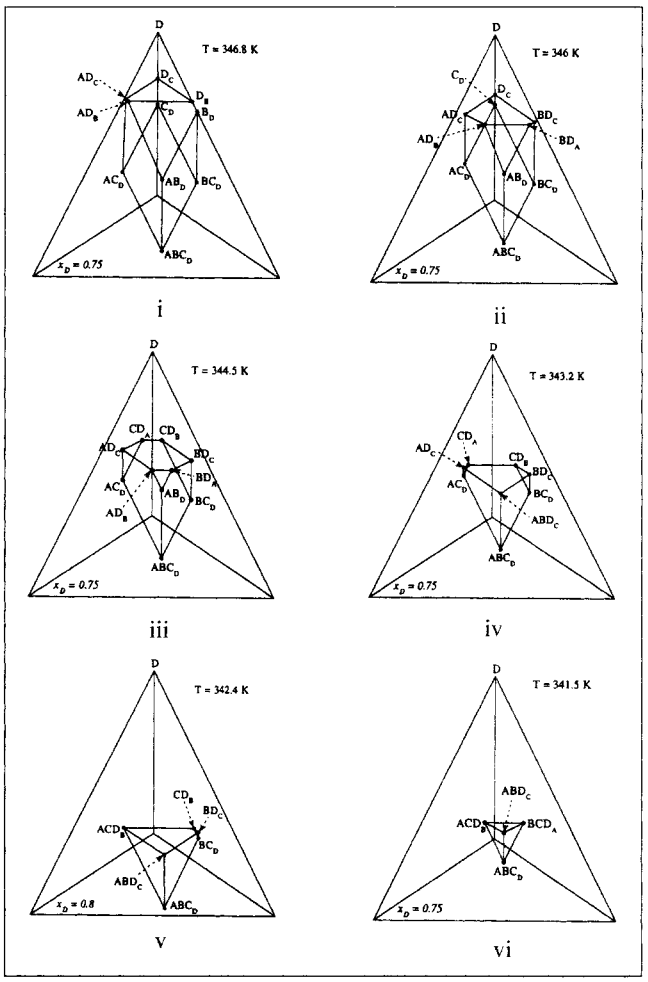

Figure 12. Evolution of saturation varieties for Example 1 (continued).

At 390 K, all the edges $\in E_{PT}^{M}$ are unidirectional. Therefore, the saturation variety matrix can be derived from Eqs. 13 and 14. This matrix is shown in Figure 10a. As before, the saturation varieties can be identified by reading across the rows of the saturation variety matrix. For example, the *A*-saturation variety can be identified by reading across row *A*-sat as the region enclosed by the edges connecting A_D, AB_D, AC_D, and ABC_D. At 346 K, we have bidirectional edges. Therefore, the saturation variety matrix is constructed by using Eq. 12. The saturation variety matrix at this temperature is shown in Figure 10b.

When a process stream is cooled gradually starting from a high temperature (at which it is in liquid phase), depending

Table 3. Data for the Quinary System (Example 2)

Pure Component Data		
	ΔH_m^0 (J/mol)	T_m (K)
A	25,000	390
B	23,000	380
C	16,000	320
D	12,000	290
E	10,000	230

Table 4. Location of Vertices of the Isothermal Isobaric Phase Diagram of Example 2 at 296 K

Vertex	x_A	x_B	x_C	x_D	x_E
A_D	0.086	0.0	0.0	0.914	0.0
A_E	0.086	0.0	0.0	0.0	0.914
B_D	0.0	0.127	0.0	0.873	0.0
B_E	0.0	0.127	0.0	0.0	0.873
C_D	0.0	0.0	0.614	0.386	0.0
C_E	0.0	0.0	0.614	0.0	0.386
AB_D	0.086	0.127	0.0	0.787	0.0
AB_E	0.086	0.127	0.0	0.0	0.787
AC_D	0.086	0.0	0.614	0.300	0.0
AC_E	0.086	0.0	0.614	0.0	0.300
BC_D	0.0	0.127	0.614	0.259	0.0
BC_E	0.0	0.127	0.614	0.0	0.259
ABC_D	0.086	0.127	0.614	0.173	0.0
ABC_E	0.086	0.127	0.614	0.0	0.173

upon its composition, different components will start to crystallize at different temperatures. The components that will precipitate first can be identified from the phase diagrams and corresponding saturation variety matrices. For example, let us consider a process stream P with the following composition: $x_A = 0.0650$, $x_B = 0.0813$, $x_C = 0.0163$, and $x_D = 0.8374$. Let us revisit Figure 3 where the location of this stream is plotted on the three polythermal projections of Figures 3b, 3c, and 3d. On the *ABC* projection (Figure 3b), P appears to lie on the *A*-saturation variety, the *B*-saturation variety, or the *AB*-double saturation variety. Also, the *D*-saturation variety is not represented. Therefore, this stream could be within the *D*-saturation variety. We need to look at the location of this stream on the remaining projections to determine the saturation variety it lies within without ambiguity. The *ABD* projection (Figure 3c) and the *ACD* projection (Figure 3d) show that stream P lies within the *A*-saturation variety only. Therefore, if we start cooling this stream from a high temperature, *A* is the first component that will be supersaturated and will start to crystallize.

Now let us consider the isothermal cut at 346 K (Figure 9). On all projections, the *A*-saturation variety comprises all the edges that connect the vertices that have *A* as a saturated component. The region formed by extending all these vertices back to the *A*-vertex, indicates the region where the solution is supersaturated with *A*. If a stream composition lies within this region on all Jänecke projections of the isothermal cut, it will be supersaturated with *A*. The *A*-supersaturation region is shown by the shaded region. Stream P lies within the region although it is not shown in Figures 9a and 9b because of truncation.

Table 5. Location of Vertices of the Isothermal Isobaric Phase Diagram of Example 2 at 310 K

Vertex	x_A	x_B	x_C	x_D	x_E
A_D	0.137	0.0	0.0	0.863	0.0
A_E	0.137	0.0	0.0	0.0	0.863
B_C	0.0	0.193	0.807	0.0	0.0
B_D	0.0	0.193	0.0	0.807	0.0
B_E	0.0	0.193	0.0	0.0	0.807
C_B	0.0	0.176	0.824	0.0	0.0
C_D	0.0	0.0	0.824	0.176	0.0
C_E	0.0	0.0	0.824	0.0	0.176
AB_C	0.137	0.193	0.670	0.0	0.0
AB_D	0.137	0.193	0.0	0.670	0.0
AB_E	0.137	0.193	0.0	0.0	0.670
AC_B	0.137	0.039	0.824	0.0	0.0
AC_D	0.137	0.0	0.824	0.039	0.0
AC_E	0.137	0.0	0.824	0.0	0.039

Evolution of Saturation Varieties. In this system, the temperature at the vertices $\in V_P^M$ falls in the order *A* ($T = 470$ K), *B*, *C*, *AB*, *AC*, *BC*, *ABC*, *D*, *AD*, *BD*, *CD*, *ABD*, *ACD*, *BCD*, *ABCD* ($T = 339.87$ K) (see Table 1). Above 470 K, the system is in liquid phase and below 339.87 K it comprises a mixture of solid *A*, *B*, *C*, and *D*. We have already seen the phase behavior at two intermediate temperatures (346 K and 390 K). Now let us observe how various saturation varieties evolve as the temperature decreases from 470 K to 339.87 K.

Figures 11 and 12 show this evolution of saturation varieties. At $T = 440$ K (between *C* and *AB*), *A*, *B*, and *C* can exist in solid phase. Edges connecting vertices A_B, A_C, and A_D bound the solubility surface of *A* (*A*-saturation variety). Similarly, edges connecting B_A, B_C, and B_D bound the *B*-saturation variety and the edges connecting C_A, C_B, and C_D bound the *C*-saturation variety. These saturation varieties represent quaternary solutions saturated with *A*, *B*, and *C* respectively. At this temperature, these saturation varieties

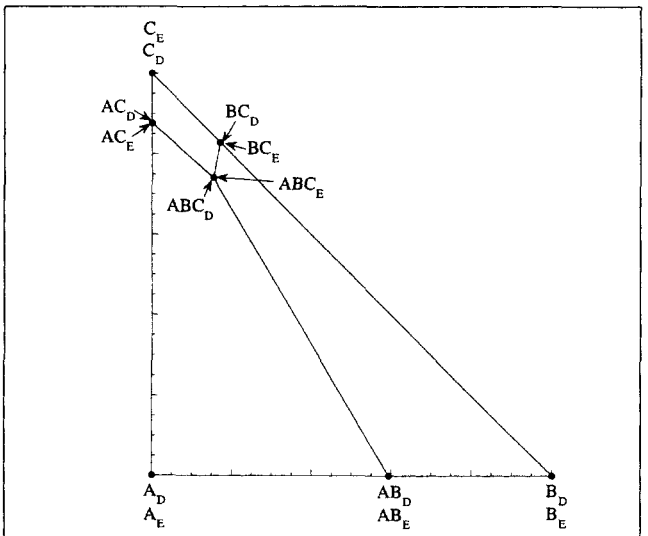

	A_D	A_E	B_D	B_E	C_D	C_E	AB_D	AB_E	AC_D	AC_E	BC_D	BC_E	ABC_D	ABC_E
A_D	0	1	0	0	0	0	1	0	1	0	0	0	0	0
A_E	1	0	0	0	0	0	0	1	0	1	0	0	0	0
B_D	0	0	0	1	0	0	1	0	0	0	1	0	0	0
B_E	0	0	1	0	0	0	0	1	0	0	0	1	0	0
C_D	0	0	0	0	0	1	0	0	1	0	1	0	0	0
C_E	0	0	0	0	1	0	0	0	0	1	0	1	0	0
AB_D	0	0	0	0	0	0	0	1	0	0	0	0	1	0
AB_E	0	0	0	0	0	0	1	0	0	0	0	0	0	1
AC_D	0	0	0	0	0	0	0	0	0	1	0	0	1	0
AC_E	0	0	0	0	0	0	0	0	1	0	0	0	0	1
BC_D	0	0	0	0	0	0	0	0	0	0	0	1	1	0
BC_E	0	0	0	0	0	0	0	0	0	0	1	0	0	1
ABC_D	0	0	0	0	0	0	0	0	0	0	0	0	0	1
ABC_E	0	0	0	0	0	0	0	0	0	0	0	0	1	0

Figure 13. Solvent-less projection and adjacency matrix of the isothermal isobaric phase diagram of Example 2 at 296 K.

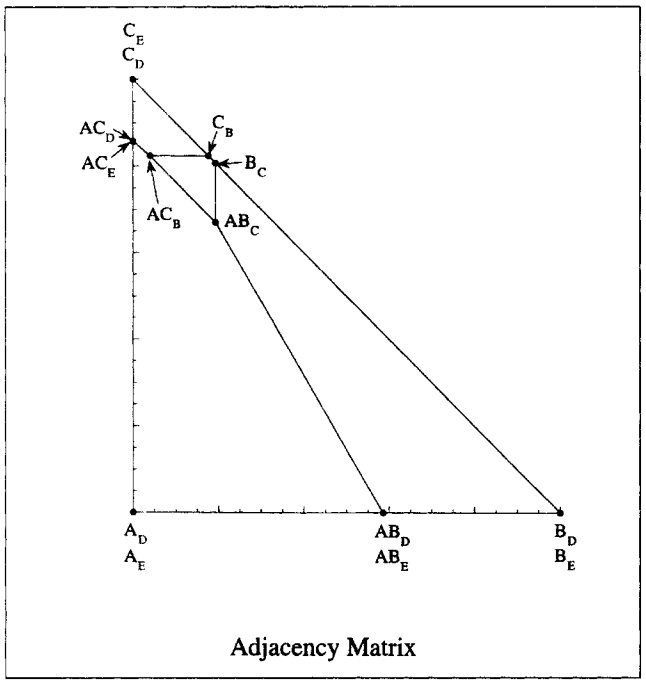

Adjacency Matrix

	A_D	A_E	B_C	B_D	B_E	AB_C	AB_D	AB_E	C_B	C_D	C_E	AC_B	AC_D	AC_E
A_D	0	1	0	0	0	0	1	0	0	0	0	0	1	0
A_E	1	0	0	0	0	0	0	1	0	0	0	0	0	1
B_C	0	0	0	1	1	1	0	0	0	0	0	0	0	0
B_D	0	0	1	0	1	0	1	0	0	0	0	0	0	0
B_E	0	0	1	1	0	0	0	1	0	0	0	0	0	0
AB_C	0	0	0	0	0	0	1	1	0	0	0	1	0	0
AB_D	0	0	0	0	0	1	0	1	0	0	0	0	0	0
AB_E	0	0	0	0	0	1	1	0	0	0	0	0	0	0
C_B	0	0	0	0	0	0	0	0	0	1	1	1	0	0
C_D	0	0	0	0	0	0	0	0	1	0	1	0	1	0
C_E	0	0	0	0	0	0	0	0	1	1	0	0	0	1
AC_B	0	0	0	0	0	1	0	0	0	0	0	0	1	1
AC_D	0	0	0	0	0	0	0	0	0	0	0	1	0	1
AC_E	0	0	0	0	0	0	0	0	0	0	0	1	1	0

Figure 14. Solvent-less projection and adjacency matrix of the isothermal isobaric phase diagram of Example 2 at 310 K.

do not intersect. Therefore, no two solids can co-exist. At 423 K (between *AB* and *AC*), the solubility surfaces of *A* and *B* meet and their intersection, edge $AB_C - AB_D$, which runs from the *ABC* face to the *ABD* face represents the *AB*-double saturation variety. The *AB*-double saturation variety represents quaternary solutions saturated with *A* and *B*. At T = 418.5 K (between *AC* and *BC*), the *A*- and *C*-saturation varieties also intersect, forming the *AC*-double saturation variety (edge $AC_B - AC_D$). At 410 K (between *BC* and *ABC*), the *B*- and *C*-saturation varieties also intersect. Edge $BC_A - BC_D$ represents the *BC* double saturation variety. At this temperature, the ternary system *A*, *B*, and *C* can still exist in liquid phase (within the triangle formed by vertices AB_C, AC_B, and BC_A on the *ABC* face). This liquid phase region disappears as the temperature is lowered to 390 K. At 390 K (between *ABC* and *D*), as we observed before, the *AB*-, *AC*-, and *BC*-double saturation varieties meet at vertex ABC_D. This vertex represents the *ABC*-triple saturation variety (quaternary solution saturated with *A*, *B*, and *C*). As the temperature falls further down to 348.5 K (between *D* and *AD*), component *D* is not limited to the liquid phase anymore as the temperature is below its melting point and the *D*-saturation variety also appears. At 346.8 K (between *AD*

(a) T = 296 K

	A_D	A_E	B_D	B_E	C_D	C_E	AB_D	AB_E	AC_D	AC_E	BC_D	BC_E	ABC_D	ABC_E
A-sat	1	1	0	0	0	0	1	1	1	1	0	0	1	1
B-sat	0	0	1	1	0	0	1	1	0	0	1	1	1	1
C-sat	0	0	0	0	1	1	0	0	1	1	1	1	1	1
AB-double sat	0	0	0	0	0	0	1	1	0	0	0	0	1	1
AC-double sat	0	0	0	0	0	0	0	0	1	1	0	0	1	1
BC-double sat	0	0	0	0	0	0	0	0	0	0	1	1	1	1
ABC-triple sat	0	0	0	0	0	0	0	0	0	0	0	0	1	1

(b) T = 310 K

	A_D	A_E	B_C	B_D	B_E	AB_C	AB_D	AB_E	C_B	C_D	C_E	AC_B	AC_D	AC_E
A-sat	1	1	0	0	0	1	1	1	0	0	0	1	1	1
B-sat	0	0	1	1	1	1	1	1	0	0	0	0	0	0
C-sat	0	0	0	0	0	0	0	0	1	1	1	1	1	1
AB-double sat	0	0	0	0	0	1	1	1	0	0	0	0	0	0
AC-double sat	0	0	0	0	0	0	0	0	0	0	0	1	1	1

Figure 15. Saturation variety matrices for the isothermal isobaric phase diagrams of Example 2.

and *BD*), the *D*-saturation variety intersects with the *A*-saturation variety to form the *AD*-double saturation variety (edge $AD_B - AD_C$). As the temperature falls further, the *BD*-double saturation variety appears at 346 K (between *BD* and *CD*), and the *CD*-double saturation variety appears at 344.5 K (between *CD* and *ABD*). At these temperatures, the ternary system *A*, *B*, and *D* can still exist in liquid phase (within the triangle formed by vertices AB_D, AD_B, and BD_A on the *ABD* face). This liquid phase region disappears as the temperature is lowered to 343.2 K (between *ABD* and *ACD*). At this temperature, the *AB*-, *AD*-, and *BD*-double saturation varieties meet to form the *ABD*-triple saturation variety (vertex ABD_C). At 342.4 K (between *ACD* and *BCD*), the *ACD*-triple saturation variety (vertex ACD_B) also appears. At the yet lower temperature of 341.5 K (between *BCD* and *ABCD*), the *BCD*-triple saturation variety (vertex BCD_A) appears. At this temperature, the liquid phase is confined entirely within the tetrahedron. The compositions of all faces of the tetrahedron represent solid mixtures. As the temperature is lowered further, the four vertices, representing the triple

Table 6. Additional Information for the Quinary System of Example 2

Feed Composition		Boiling points at 1 atm	
x_A	0.3609	*A*	540 K
x_B	0.1579	*B*	500 K
x_C	0.0323	*C*	455 K
x_D	0.4489	*D*	430 K
		E	268 K

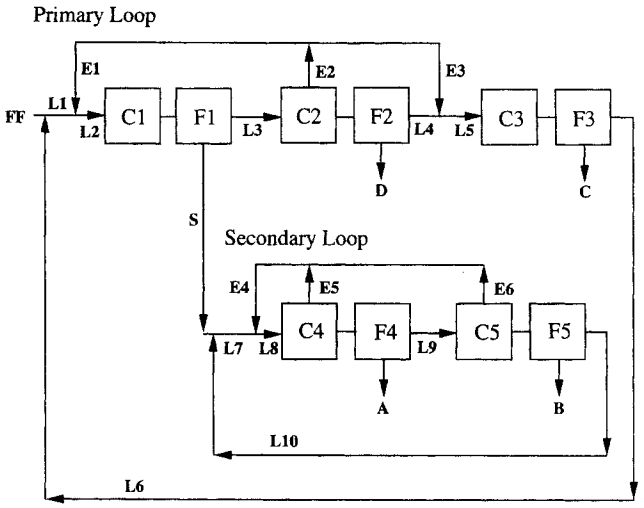

Figure 16. Flow sheet for separation of *A*, *B*, *C*, and *D* from the quinary system of Example 2.

saturation varieties approach each other until they meet at 339.87 K and the liquid phase disappears completely for $T <$ 339.87 K. It should be noted that the evolution pattern is based on the order in which the temperature associated with the vertices falls. A different pattern will be observed for a different order.

Example 2: quinary system

This example illustrates the case of multiple solvents. The system under consideration comprises five components: *A*, *B*, *C*, *D*, *E*. The only data available are the pure component data (Table 3). Therefore, for all calculations, we will assume that the system behaves ideally.

Let us develop the isothermal isobaric phase diagrams at two temperatures, 296 K and 310 K. The vertices and their locations at these temperatures are listed in Tables 4 and 5, respectively. At both these temperatures, we have two solvents *D* and *E*. Therefore, we can plot the isothermal isobaric phase behavior as one Jänecke projection. These projections and their adjacency matrices are shown in Figures 13 and 14. Figure 15 shows the saturation variety matrices.

It is interesting to note that due to the presence of multiple solvents, none of the vertices of the digraph represents a quinary solution. At all vertices, the unsaturated component is either *D* or *E*. The vertices with the same saturated components (for example, AB_D and AB_E on Figure 13) and the edges connecting them (for example, AB_D–ABC_D and AB_E–ABC_E on Figure 13) coincide on the solvent-less projections for this ideal system. They may not coincide for nonideal systems. It is interesting to note that the *BC*-double saturation and the *ABC*-triple saturation varieties do not exist at 310 K. These varieties appear only when the temperature is decreased below the temperature of the *ABC* ternary eutectic point (303.85 K).

Table 7. Crystallizer Operating Temperatures for the Process of Figure 16

Crystallizer	Operating Temperature
Primary Loop	
C1	223.68 K
C2	259.71 K
C3	244.69 K
Secondary Loop	
C4	270 K
C5	340 K

Table 8. Stream Data for the Process of Figure 16*

Stream	*A*	*B*	*C*	*D*	*E*	Total Flow
FF	0.3609	0.1579	0.0323	0.4489	0.0	1.0
L1	0.3769	0.1884	0.3015	1.1307	0.7161	2.7136
L2	0.3769	0.1884	0.3015	1.1307	3.4674	5.4649
L3	0.0160	0.0305	0.3015	1.1307	3.4674	4.9461
L4	0.0160	0.0305	0.3015	0.6818	0.1884	1.2182
L5	0.0160	0.0305	0.3015	0.6818	0.7161	1.7459
L6	0.0160	0.0305	0.2692	0.6818	0.7161	1.7136
L7	0.9618	0.9518	0.0	0.0	0.4745	2.3881
L8	0.9618	0.9518	0.0	0.0	27.4317	29.3453
L9	0.6009	0.9518	0.0	0.0	16.9421	18.4948
L10	0.6009	0.7938	0.0	0.0	0.4746	1.8693
E1	0.0	0.0	0.0	0.0	2.7513	2.7513
E2	0.0	0.0	0.0	0.0	3.2790	3.2790
E3	0.0	0.0	0.0	0.0	0.5277	0.5277
E4	0.0	0.0	0.0	0.0	26.9572	26.9572
E5	0.0	0.0	0.0	0.0	10.4896	10.4896
E6	0.0	0.0	0.0	0.0	16.4676	16.4676
S	0.3609	0.1579	0.0	0.0	0.0	0.5188
A	0.3609	0.0	0.0	0.0	0.0	0.3609
B	0.0	0.1579	0.0	0.0	0.0	0.1579
C	0.0	0.0	0.0323	0.0	0.0	0.0323
D	0.0	0.0	0.0	0.4489	0.0	0.4489

*All flows are normalized with the fresh feed (FF) flow.

Applications

As these examples illustrate, the main advantage of the framework is the ease with which it allows the user to visualize and study the phase behavior of high-dimensional systems. The phase diagrams generated can be used to aid the experimental measurement of phase behavior and to synthesize crystallization processes. In the discussion on location of vertices and calculation of edges, we have provided suggestions on how to use the framework for experimental studies. In this section, we discuss in detail its application to process synthesis.

We consider the quinary system of Example 2. The objective is to separate a mixture of *A*, *B*, *C*, and *D* into pure components using solvent *E*. The additional information about the system is summarized in Table 6. Note that our intention is not to present a formal procedure for crystallization process synthesis. Instead, our focus is on showing how the phase diagrams (appropriate projections and cuts) can be used to develop a feasible process flow sheet.

One feasible flow sheet is shown in Figure 16. The separation train in this flow sheet is divided into two loops. In the primary loop, the fresh feed (FF) is mixed with the recycle stream (L6) and solvent stream (E1) to form the feed to the first crystallizer (L2). This crystallizer is operated as a cooling

crystallizer. A mixture of solid A and solid B is separated and is then sent to the secondary loop for separation. The mother liquor (L3) is then sent to the second crystallizer. Solid D is separated in this crystallizer which operates as an evaporative crystallizer. The solvent stream (E2) is divided into two parts. The first part (E1) is sent to the inlet of the first crystallizer and the second part (E3) is mixed with the mother liquor (L4) to form the feed to the third crystallizer (L5). The third crystallizer also operates as a cooling crystallizer and separates solid C. The mother liquor (L6) is sent back as the

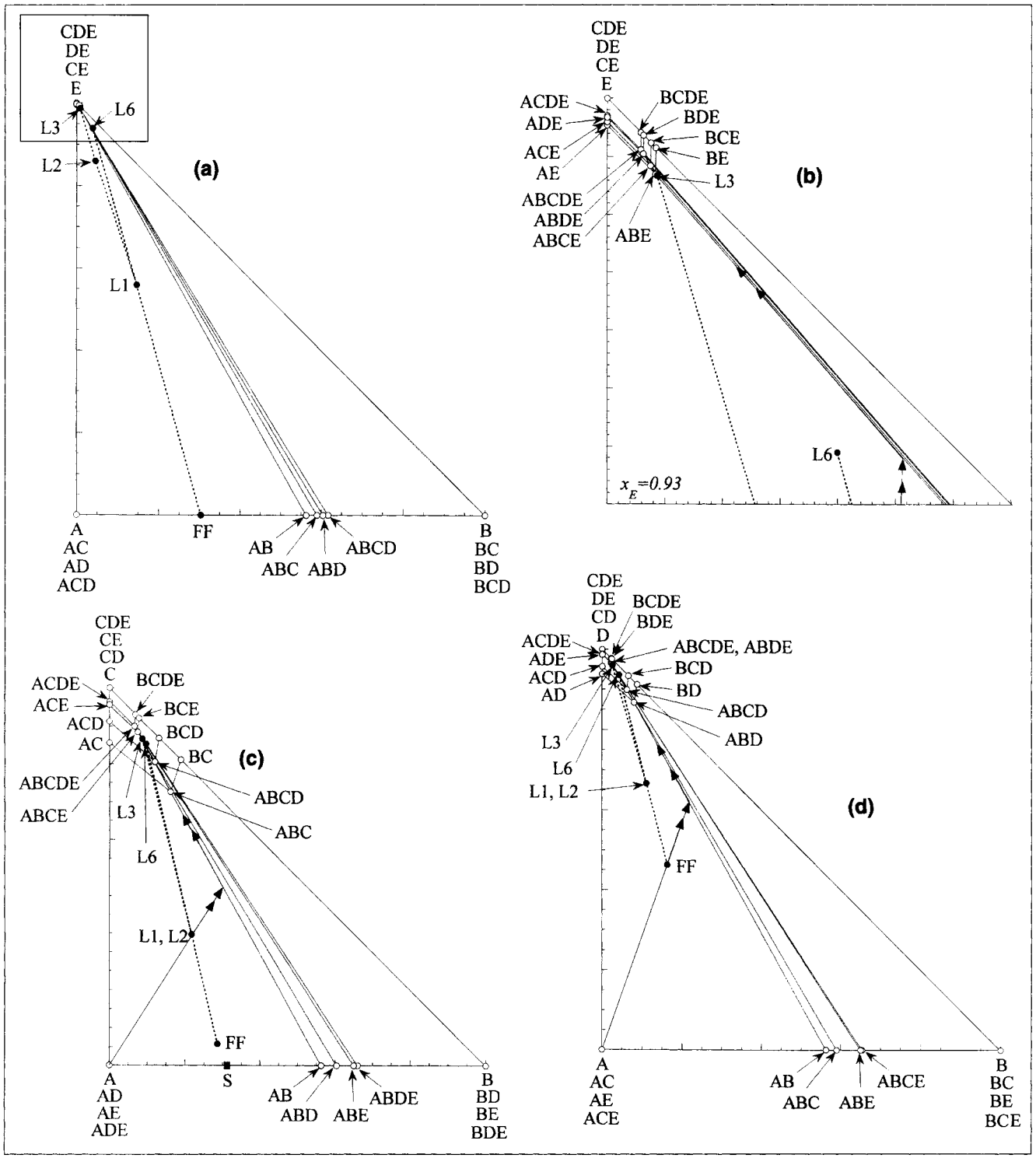

Figure 17. Polythermal projections depicting the operation of crystallizer C1.

(a) *ABE* projection; (b) blowup of the top portion (the box in (a)) of the *ABE* projection; (c) *ABC* projection; (d) *ABD* projection.

recycle stream. In the secondary loop, the mixture of A and B is mixed with the recycle stream for this loop (L10) and the solvent (E4) to form the feed stream (L8). This stream is sent to a series of two crystallizers, both operated in the evaporative mode. A is separated in the first crystallizer, and B is separated in the second. The mother liquor from the second crystallizer (L10) is sent back as the recycle stream and the solvent streams (E5 and E6) are sent back to the inlet of the first crystallizer. The temperatures used for each crystallizer are listed in Table 7 and the stream data are listed in Table 8. Note that this flow sheet is simply one of many feasible alternatives. It may not be the optimum both in terms of the flow sheet structure and operating conditions. Many other alternatives can be developed for this separation task. Let us now turn our attention to how we can use the phase diagrams to aid in constructing this flow sheet.

The operation of crystallizer C1 is depicted on the phase diagrams in Figure 17. Figures 17a, 17c, and 17d show three polythermal projections, *ABE*, *ABC*, and *ABD*, respectively, of the isobaric phase diagram. Figure 17b shows a blowup of the top portion of the *ABE* projection. The crystallizer operation is shown with filled circles and dotted material balance

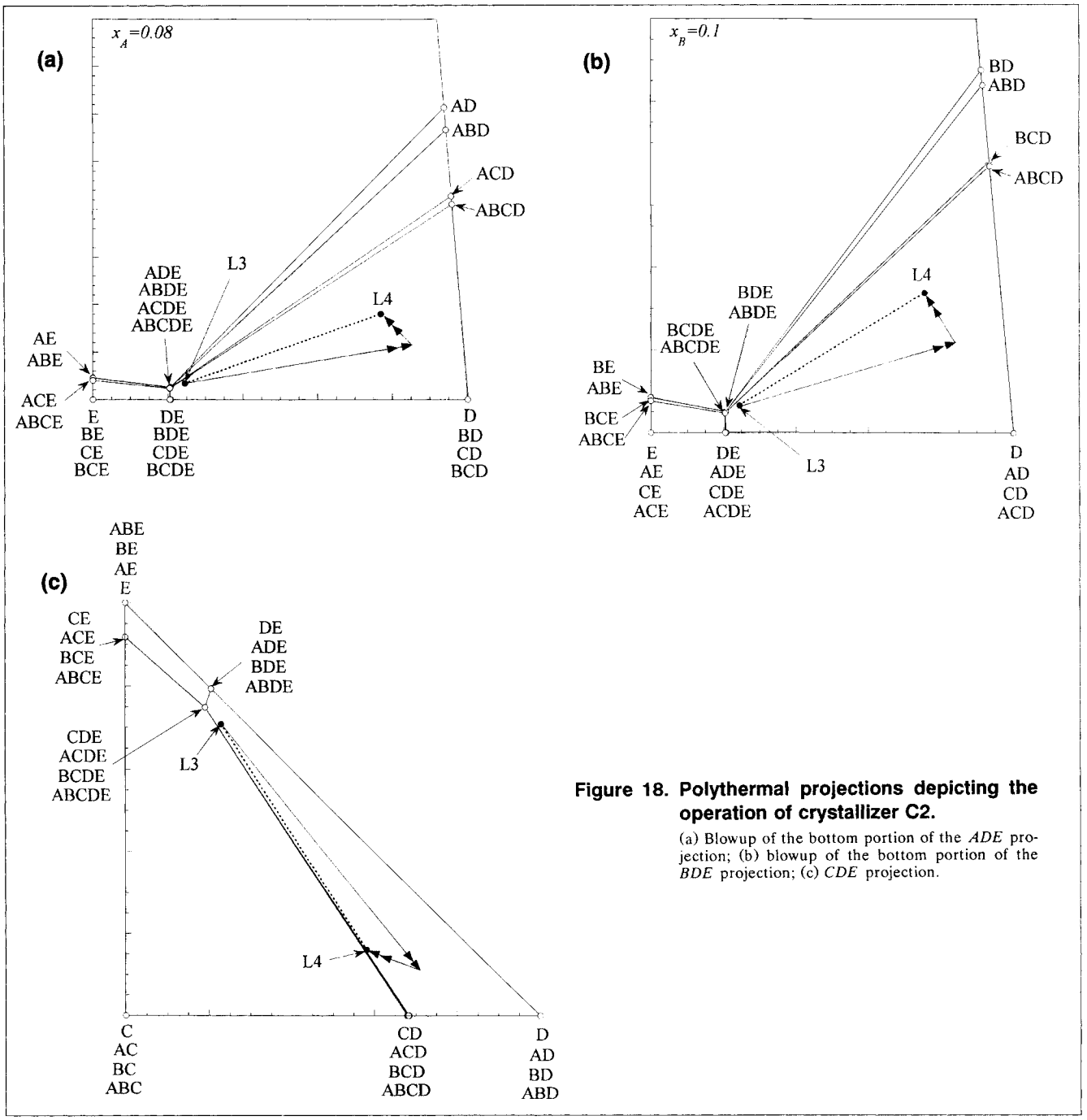

Figure 18. Polythermal projections depicting the operation of crystallizer C2.

(a) Blowup of the bottom portion of the *ADE* projection; (b) blowup of the bottom portion of the *BDE* projection; (c) *CDE* projection.

lines (the same convention is followed in the rest of the figures). The feed stream to this crystallizer, stream L2, lies on the *A*-saturation variety on projection *ABE*. Therefore, we may expect *A* to precipitate from this stream as we gradually cool it down from a high temperature. We cannot be certain, however, as *C*-saturation, *D*-saturation, and *CD*-double saturation varieties are not represented on this projection and stream L2 could very well be on any of these saturation varieties. To ensure this is not the case, we need the two additional projections, *ABC* and *ABD*. In both projections L2 lies in the *A*-saturation region. Therefore, our conjecture is indeed true. If we cool stream L2 further, it reaches the *AB*-double saturation variety (see the double-headed arrow in Figures 17b, 17c, and 17d) and moves along this surface while precipitating *A* and *B* simultaneously until it reaches a triple saturation variety. The triple saturation variety it will first reach is the *ABD*-triple saturation variety. The temperature at which stream L2 is barely saturated with *D* is 223.68 K. To

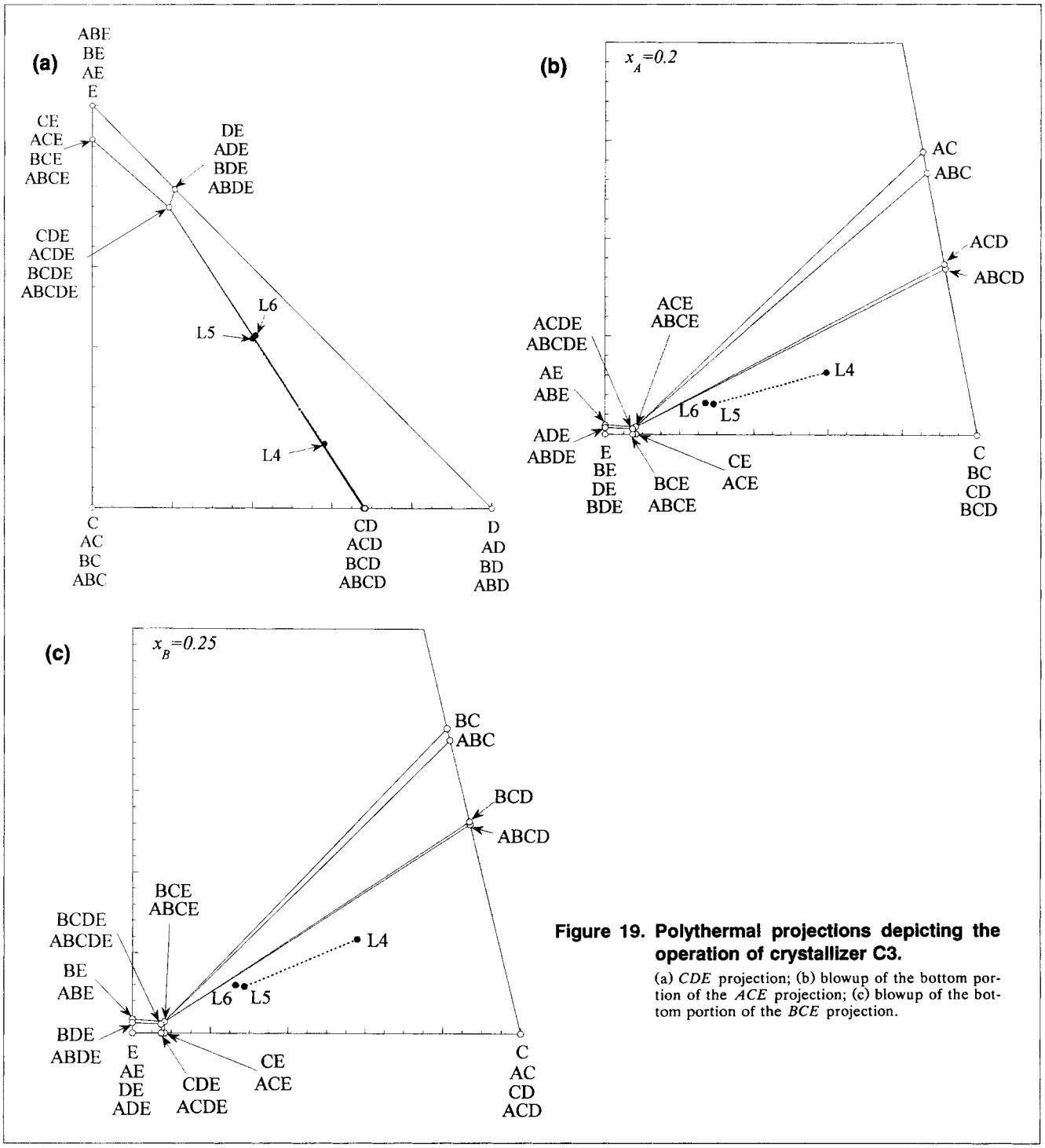

Figure 19. Polythermal projections depicting the operation of crystallizer C3.

(a) *CDE* projection; (b) blowup of the bottom portion of the *ACE* projection; (c) blowup of the bottom portion of the *BCE* projection.

separate the most A and B from L2, crystallizer C1 has to be operated at this temperature. The composition of stream S (solid A and solid B) is shown as a filled square on Figure 17c.

Figure 18 shows the operation of crystallizer C2. Figures 18a, 18b, and 18c show the *ADE*, *BDE*, and *CDE* projections of the polythermal diagram. For the sake of clarity, Figures 18a and b show only the bottom portions of the projection. (Note that the length of the y-axis is not unity.) From the *ADE* projection, we observe that if we remove solvent E from stream L3, we can push it back into the D-saturation region and then use appropriate temperature to precipitate D from the solution (see double-headed arrows). To make sure of this fact, we have to study the *BDE* and the *CDE*

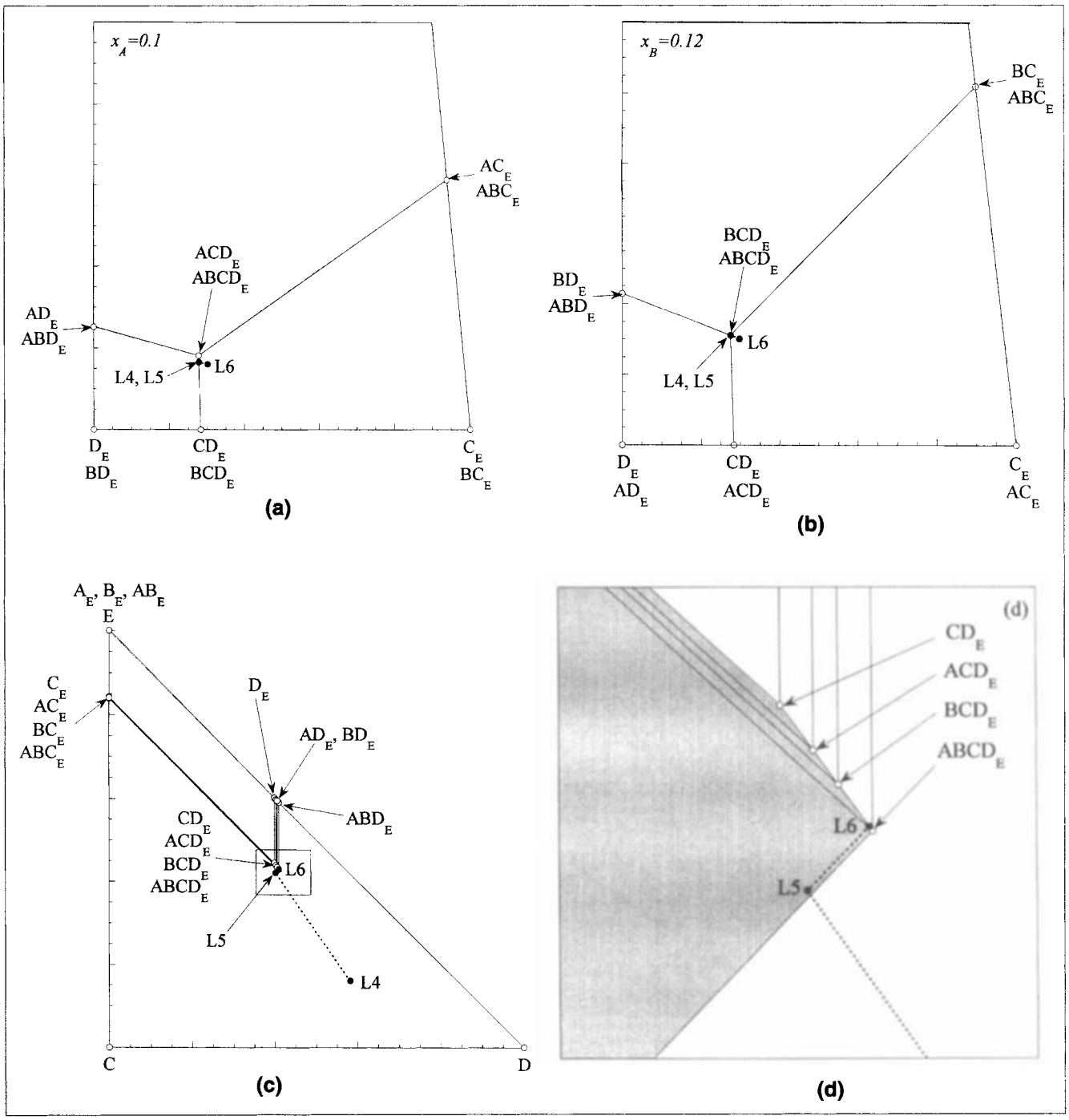

Figure 20. Isothermal cuts depicting the operation of crystallizer C3.

(a) Blowup of the bottom portion of the *ACD* projection; (b) blowup of the bottom portion of the *BCD* projection; (c) *CDE* projection; (d) blowup of the box in the *CDE* projection.

projections as well. From these three projections, it is clear that this can be done. The mother liquor L4 is close to the *CD*-double saturation variety. To remove the maximum amount of *D* from L3, we operate C2 at a temperature where component *C* is barely saturated (259.71 K). This temperature is comparable to the boiling point of the solvent at 1 atm. Therefore, we combine the operations of solvent removal and crystallization into one single evaporative crystallizer.

The operation of crystallizer C3 is shown in Figure 19. Figures 19a, 19b, and 19c show the *CDE*, *ACE*, and *BCE* projections, respectively. Again for the sake of clarity, Figures 19a and 19b show the blowups of the bottom portions of the projection. From Figure 19a, we see that we can move the stream L4 which is in the *D*-saturation region, to stream L5 which is situated in the *C*-saturation region by addition of solvent *E*. We have to make sure that L5 is indeed in the *C* saturation region by using the other two projections. The stream L5 can now be cooled to a temperature at which any one of the remaining components approaches saturation (244.69 K). The mother liquor L6 is recycled back to the first crystallizer as shown in Figure 17.

Let us now consider what happens at the temperature of operation of C3. Figures 20a and 20b show the *ACD*, and *BCD* projections, and Figures 20c and 20d show the *CDE* projection of the isothermal cut at this temperature. The effect of solvent addition cannot be seen from Figures 20a and 20b as *E* is not plotted on these projections and streams L4 and L5, therefore, are at the same location. However, we can verify that at this temperature they are not saturated with *A* and *B*. We can see the effect of solvent addition from the *CDE* projection (Figures 20c and 20d). Figure 20d shows a blowup of the box in Figure 20c. The shaded region is a part of the *C*-supersaturation region (identified from the saturation variety matrix) on this projection. We can see how the solvent addition brings the stream L4 into the *C*-saturation region. Also the mother liquor L6 is close to the *BCD*-triple saturation variety.

In the secondary loop, the task is to separate the binary mixture of *A* and *B* into pure components using solvent *E* (note that any other solvent may also be used). Figure 21 shows the isothermal cuts at the temperatures of operation of C4 and C5. The first crystallizer C4 is operated at the colder temperature (270 K). The isothermal cut at this temperature is shown with hollow squares. The feed stream L8 lies on the *A*-saturation variety (edge $A_E - AB_E$). As we remove solvent *E* from this stream, *A* crystallizes and the liquid composition moves along the *A*-saturation variety until we are very close to the *AB*-double saturation variety (vertex AB_E). For maximum separation of *A*, the amount of solvent removed is such that the mother liquor (stream L9) is extremely close to the AB_E vertex at 270 K. The second crystallizer C5 is operated at a higher temperature (340 K). The isothermal cut at this temperature is shown with hollow spheres. The feed to C5 (stream L9) is unsaturated at this temperature. As we remove solvent *E* from this stream, its composition moves along the dotted line until it reaches the *B*-saturation variety (edge $B_E - AB_E$) and then along this edge (as shown by the arrow) while crystallizing *B*. For maximum separation of *B*, the amount of solvent removed is such that the mother liquid (stream L10) is extremely close to the AB_E vertex at 340 K.

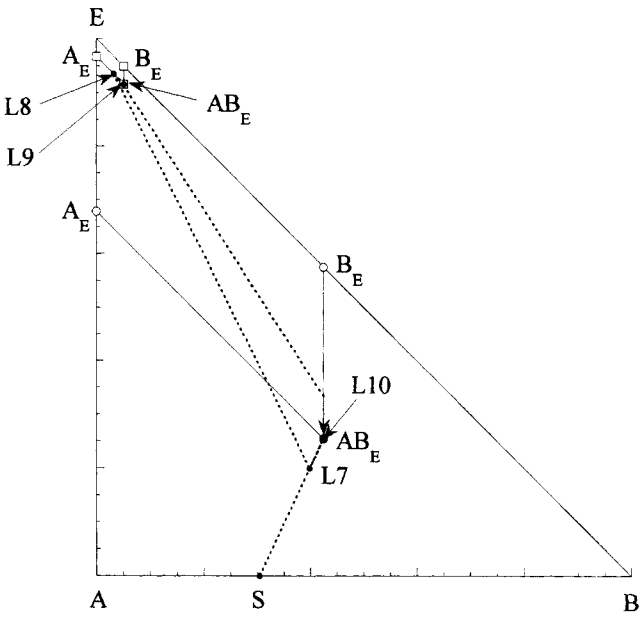

Figure 21. Isothermal cuts depicting the operation of crystallizers C4 and C5.

The solvent streams and stream L10 are recycled. Both the crystallizer are operated in the evaporative mode as the boiling point of the solvent at 1 atm is lower than the operating temperatures.

Conclusions

Process conceptualization, a critical phase of process development, is one in which the possible flow sheets are identified. Visualization of high-dimensional solid-liquid phase diagrams is crucial in the synthesis of crystallization-based separation processes. Yet this problem has bedeviled researchers in thermodynamics and crystallization for a long time. For systems that cannot be presented on a 3-D plot, it is hard to communicate the geometrical features even if the numerical information is available. To meet this need, a framework to systematize the task of representing the phase behavior of multicomponent systems has been developed.

The geometry of the phase diagram in high-dimensional composition space is captured in a digraph as represented by its various associated matrices. A systematic procedure allows the user to zoom in on any part of the phase diagram as desired to view the corresponding cuts and projections. Despite the infeasibility of viewing it as a whole, the user gains a mental picture of the phase diagram in its entirety.

Only minimum information is required for using the framework, namely, the pure component melting points and heats of fusion. It is true that not all solid-liquid phase behaviors are simple-eutectic in nature and can be highly nonideal. However, the present procedure can be used to provide a basic structure for the phase diagram, which can be used to guide the experimental efforts for generating additional information.

Although this article discusses only molecular systems, the framework is generic in nature. It can be used, with minor

modifications, for the representation of phase diagrams of reactive, compound forming, and ionic systems. Effort in this direction is under way. Efforts are also under way to implement this framework in form of a software tool for generation and visualization of high-dimensional phase diagrams.

Acknowledgment

We express our appreciation to the National Science Foundation, grant No. CTS-9908667, for support of this research.

Notation

$A = (a_{ij})$ = adjacency matrix
c = number of components
e_{ij} = edge $\in E$ joining vertices v_i and v_j
E = set of edges of a digraph
f = degrees of freedom
G = digraph
$\Delta H^o_{m,i}$ = heat of fusion of component i
I = identity matrix
i, j, k, n = indices
P = minimum number of figures for complete representation of phase behavior
Q = number of equations
R = universal gas constant
s = number of solvents
$S = (s_{ij})$ = saturation variety matrix
T = temperature
$T_{m,i}$ = melting point of component i
v_i = vertex $\in V$
V = set of vertices of a digraph
W = number of independent intensive variables
x_i = mole fraction of component i
γ_i = liquid phase activity coefficient of component i

Subscripts

min = minimum value
max = maximum value
e_{ij} = along edge e_{ij}
P = at constant pressure
T = at constant temperature
v_i = on vertex v_i

Superscripts

M = molecular system
sat = at saturation

Literature Cited

Berry, D. A., S. R. Dye, and K. M. Ng, "Synthesis of Drowning-Out Crystallization-Based Separations," *AIChE J.*, **43**, 91 (1997).

Berry, D. A., and K. M. Ng, "Synthesis of Reactive Crystallization Processes," *AIChE J.*, **43**, 1737 (1997).

Biggs, N., *Algebraic Graph Theory*, 2nd ed., University Press, Cambridge (1993).

Cisternas, L. A., and D. F. Rudd, "Process Designs for Fractional Crytallization from Solution," *Ind. Eng. Chem. Res.*, **32**, 1993 (1993).

Dye, S. R., and K. M. Ng, "Bypassing Eutectics with Extractive Crystallization: Design Alternatives and Trade-offs," *AIChE J.*, **41**, 1456 (1995a).

Dye, S. R., and K. M. Ng, "Fractional Crytallization: Design Alternatives and Trade-offs," *AIChE J.*, **41**, 2427 (1995b).

Fitch, B., "How to Design Fractional Crytallization Processes," *Ind. Eng. Chem. Res.*, **62**(12), 6 (1970).

Hasse, R., and H. Schönert, *Solid-Liquid Equilibrium*, Pergamon, New York (1969).

Mullin, J. W., *Crystallization*, 3rd ed., Butterworth-Heinemann, Oxford (1993).

Myerson, A. S., ed., *Handbook of Industrial Crystallization*, Butterworth-Heinemann, Boston (1993).

Rousseau, R. W., ed., *Crystallization*, Kirk-Othmer Encyclopedia of Chemical Technology, 4th ed., Vol. 7, Wiley Interscience, New York, p. 683 (1994).

Pressly, T. G., and K. M. Ng, "Process Boundary Approach to Separations Synthesis," *AIChE J.*, **45**, 1939 (1999).

Ricci, J. E., *The Phase Rule and Heterogeneous Equilibrium*, D. Van Nostrand Co., New York (1993).

Thomsen, K., P. Rasmusen, and R. Gani, "Simulation and Optimization of Fractional Crystallization Processes," *Chem. Eng. Sci.*, **53**, 1551 (1998).

Appendix: Minimum Number of Figures for Complete Representation of Phase Behavior

Consider an n-dimensional system. Let the minimum number of ternary projections needed to completely represent the system be P. The representation of the system is complete if each coordinate appears at least once with each of the remaining coordinates.

Case 1: Odd n

To minimize P while completely representing the system, the projections can be selected in the following manner:

- Select one coordinate and divide the rest into pairs.
- Combine the selected coordinate with each pair to form a ternary projection.
- Combine each coordinate of the first pair with each of the remaining pairs (second onwards) to form a ternary projection.
- Combine each coordinate of the second pair with each of the remaining pairs (third onwards) to form a ternary projection.
- Repeat and stop when each coordinate of the last but one pair is combined with the last pair.

The number of projections thus obtained is

$$P = \frac{(n-1)}{2} + \sum_{k=2}^{\frac{(n-1)}{2}} [n-(2k-1)]$$

$$= \frac{(n-1)^2}{2} - \sum_{k=1}^{\frac{(n-1)}{2}} (2k-1)$$

$$= \frac{(n-1)^2}{4} \qquad \text{(A1)}$$

Case 2: Even n

In this case the projections can be selected as follows:

- Divide the coordinates into pairs.
- Select one pair. Neglect one of the coordinates from this pair and follow the steps in case 1 for the other coordinate.
- Combine the neglected coordinate with the remaining groups.
- Combine the neglected coordinate with the other coordinate from its pair and any other coordinate from the remaining pairs.

This leads to

$$P = \frac{(n-2)^2}{4} + \frac{(n-2)}{2} + 1$$

$$= \frac{(n-1)^2}{4} + \frac{3}{4} \qquad \text{(A2)}$$

Combining Eqs. A1 and A2, we have

$$P = \frac{(n-1)^2}{4} + k, \qquad k = \begin{cases} 0 & \text{if } n \text{ is odd,} \\ \dfrac{3}{4} & \text{if } n \text{ is even.} \end{cases} \qquad \text{(A3)}$$

For polythermal projections and isothermal cuts, $n = c$, and for Jänecke projections of the isothermal cut, $n = c - s$ (s is the number of solvents).

Manuscript received Jan. 10, 2000, and revision received May 4, 2000.